REPORT DOCUMENTATION PAGE

READ INSTRUCTIONS BEFORE COMPLETING FORM

1. REPORT NUMBER

2. GOVT ACCESSION NO.

3. RECIPIENT'S CATALOG NUMBER

4. TITLE (and Subtitle)
DETERMINATION OF OPTIMUM FIN PLANFORM AND AIRFOIL SECTION FOR MINIMIZING FIN HINGE MOMENT

5. TYPE OF REPORT & PERIOD COVERED
Final Report
12/1/81 to 12/31/82

6. PERFORMING ORG. REPORT NUMBER
NEAR TR 286

7. AUTHOR(s)
Frederick K. Goodwin and Jack N. Nielsen

8. CONTRACT OR GRANT NUMBER(s)
N00014-81-C-0267

9. PERFORMING ORGANIZATION NAME AND ADDRESS
Nielsen Engineering & Research, Inc.
510 Clyde Avenue
Mountain View, CA 94043

10. PROGRAM ELEMENT, PROJECT, TASK AREA & WORK UNIT NUMBERS

11. CONTROLLING OFFICE NAME AND ADDRESS
Office of Naval Research
Arlington, VA 22217

12. REPORT DATE
February 1983

13. NUMBER OF PAGES
87

14. MONITORING AGENCY NAME & ADDRESS(if different from Controlling Office)

15. SECURITY CLASS (of this report)
Unclassified

15a. DECLASSIFICATION DOWNGRADING SCHEDULE

16. DISTRIBUTION STATEMENT (of this Report)
Approved for public release; distribution unlimited

17. DISTRIBUTION STATEMENT (of the abstract entered in Block 20, if different from Report)

18. SUPPLEMENTARY NOTES

19. KEY WORDS (Continue on reverse side if necessary and identify by block number)
Missile Airframes
All-Movable Controls
Hinge moments
Aerodynamic Forces
Supersonic Characteristics
Control Surfaces

20. ABSTRACT (Continue on reverse side if necessary and identify by block number)
This report is the technical report on the second phase of an investigation of the hinge moments of all-movable controls as utilized on cruciform missiles. In the first phase, an attempt was made to develop as general as possible a hinge-moment prediction method for speeds ranging from subsonic to hypersonic. In that work, the method was successfully applied for Mach numbers ranging from 1.3 to 3.7. In the present phase of the

20. ABSTRACT (Concluded)

investigation, the methods from phase one, with some modifications, have been used to develop a procedure for determining the optimum fin planform and airfoil section to minimize the fin hinge moment over a range of Mach numbers, angles of attack, and fin deflection angles. The Mach number range is restricted to supersonic. This report describes the further modifications made to program MISSILE2 and describes the optimization procedure. A user's manual for the computer program is presented in an appendix.

COPY NO. 81

DETERMINATION OF OPTIMUM FIN PLANFORM AND AIRFOIL SECTION FOR MINIMIZING FIN HINGE MOMENT

by

Frederick K. Goodwin and Jack N. Nielsen

NEAR TR 286
February 1983

Prepared under Contract No. N00014-81-C-0267

for

OFFICE OF NAVAL RESEARCH
Arlington, Virginia 22217

by

NIELSEN ENGINEERING & RESEARCH, INC.
510 Clyde Avenue, Mountain View, CA 94043
Telephone (415) 968-9457

SUMMARY

This report is the technical report on the second phase of an investigation of the hinge moments of all-movable controls as utilized on cruciform missiles. In the first phase, an attempt was made to develop a hinge-moment prediction method as general as possible for speeds ranging from subsonic to hypersonic. In that work, the method was successfully applied for Mach numbers ranging from 1.3 to 3.7. In the present phase of the investigation, the methods from phase one, with some modifications, have been used to develop a procedure for determining the optimum fin planform and airfoil section to minimize the fin hinge moment over a range of Mach numbers, angles of attack, and fin deflection angles. The Mach number range is restricted to supersonic. The transonic speed range cannot be handled since methods are not presently available for predicting the center-of-pressure shift due to thickness in this speed range. Experimental data are not available to assess the accuracy of the method at hypersonic speeds.

PREFACE

This technical report covers the work performed under Contract N00014-81-C-0276 from December 1, 1981 to December 31, 1982. The program is sponsored by the Office of Naval Research, Arlington, Virginia. Dr. Robert E. Whitehead is the Scientific Officer.

Support for the program was provided by Air Force Wright Aeronautical Laboratory (AFWAL), under the leadership of Mr. Vernon O. Hoehne.

TABLE OF CONTENTS

LIST OF ILLUSTRATIONS

LIST OF SYMBOLS

a	body radius on cylindrical section
$\text{Æ}R$	aspect ratio of two fins joined together at their root chords
c	local fin chord
c_{d_c}	crossflow-drag coefficient
c_r	fin root-chord length
c_t	fin tip-chord length
C_A	axial-force coefficient, axial force/$q_\infty S_R$, positive as shown in figure A.10
C_{BM_i}	root-bending-moment coefficient of the *ith* fin, root-bending moment/$q_\infty S_R \ell_R$, positive as shown in figure A.9
C_D	drag coefficient, drag/$q_\infty S_R$, positive as shown in figure A.10
C_{HM_i}	hinge-moment coefficient of the *ith* fin, hinge moment/$q_\infty S_R \ell_R$, positive as shown in figure 6 or A.9
$\lvert C_{HM_{opt}} \rvert$	magnitude of the maximum $\lvert C_{HM} \rvert$ with the hinge line in optimum position
C_L	lift coefficient, lift/$q_\infty S_R$, positive as shown in figure A.10
C_{m_x}, C_{m_y}, C_{m_z}	moments about the x,y,z axes respectively, moment/$q_\infty S_R \ell_R$, positive as shown in figure A.10
$C_{m_{x_o}}$, $C_{m_{y_o}}$, $C_{m_{z_o}}$	moments about the x_o, y_o, z_o axes respectively, moment/$q_\infty S_R \ell_R$, positive as shown in figure A.10
C_N	fin-alone normal-force coefficient, normal force/$q_\infty S_R$
C_{NF_i}	fin in presence of body normal-force coefficient for the *ith* fin, normal force/$q_\infty S_R$, positive as shown in figure A.9

C_{N_α}	normal-force-curve slope of nose, d/dα (normal force/$q_\infty S_R$)
C_P	Pressure coefficient, $(p - p_\infty)/q_\infty$
C_{RM_i}	rolling-moment coefficient due to *ith* fin, rolling moment/$q_\infty S_R \ell_R$, positive as shown in figure A.9
C_x, C_y, C_z	forces in the x,y,z directions, force/$q_\infty S_R$, positive as shown in figure A.10
$C_{x_o}, C_{y_o}, C_{z_o}$	forces in the x_o, y_o, z_o directions, force/$q_\infty S_R$, positive as shown in figure A.10
C_1, C_2	constants defined by Equation (3)
d	body diameter on cylindrical section
f	length of flat section of airfoil, see figure 1
$K_{B(C)}$	fin-body interference factor for body normal force
ℓ_R	reference length; taken equal to d
m	$1/\tan\Lambda_{LE}$
M_∞	free-stream Mach number
p	static pressure
p_∞	free-stream static pressure
q_∞	free-stream dynamic pressure
s	span of fin measured from body axis to fin tip
S_F	area of fin
S_R	reference area, taken equal to $\pi d^2/4$
t	maximum thickness of airfoil, see figure 1
V_∞	free-stream velocity
x,y,z	rolled coordinate system shown in figure A.10
x_{HL}	location of fin hinge line measured from root-chord leading edge

x_o, y_o, z_o	unrolled coordinate system shown in figure A.10
$\bar{x}$	axial location of fin center of pressure measured from root-chord leading edge
$(\Delta\bar{x})_t$	center of pressure shift due to fin thickness, positive forward
α	fin-alone angle of attack
α_c	combined angle of attack of body-canard combination
β	$\sqrt{M_\infty^2 - 1}$
γ	ratio of specific heat; $\gamma = 1.4$ for air
δ	fin deflection angle
δ_i	deflection angle of i*th* fin, $i = 1,2,3,4$; viewed from the rear at $\phi = 0$, fin 1 is on top and they are numbered counterclockwise, see figure A.10
θ_i	surface slope of i*th* section of airfoil, see figure 1
λ	taper ratio, $\lambda = c_t/c_r$
Λ_{LE}	sweep angle of fin leading edge
ϕ	roll angle of missile, positive clockwise viewed from the rear; $\phi = 0°$ has fin 1 on top

Subscripts

ℓ	lower surface of airfoil
max	maximum value
min	minimum value
nt	no thickness
u	upper surface of airfoil

1. INTRODUCTION

The determination of the fin size, planform, and airfoil section to provide a missile with adequate control while minimizing fin hinge moment has received little analytical treatment over the years. The problem has normally been studied by performing expensive and time consuming wind-tunnel testing. Since the weights of the control actuators and their power supplies are substantial, the design of a minimum hinge-moment fin would help keep this weight down.

The work described in Reference 1 was directed toward developing a method which would accurately predict, including thickness effects, the hinge moments on all-movable controls. It uses the methodology developed in References 2 and 3 and expanded upon and modified the computer program of Reference 3, MISSILE2. It was found, in Reference 1, that the canard hinge moments were well predicted at supersonic speeds except for leeward fins when strong body vortices were present. At transonic speeds, the predictions were not good. As a result of these comparisons, it is felt that the methodology exists for developing a method for determining the optimum fin planform and airfoil section for minimizing the hinge moment acting on all-movable controls at supersonic speeds. It is the purpose of this report to summarize such a method.

This work is being conducted under contract N00014-81-C-0267 from the Office of Naval Research which is supported by the Flight Dynamics Laboratory of the Air Force Wright Aeronautical Laboratories. This is Phase II of the work. The results of Phase I are documented in Reference 1.

In this report a general discussion of the problem is first presented. This is followed by an explanation of the modifications made to program MISSILE2 and an example of how the optimum hinge-line location is determined for a particular fin. Next, the procedure used to determine the optimum fin to minimize hinge

moment for a particular set of constraints is described. The last section presents some concluding remarks. The computer program is described in an appendix.

2. GENERAL CONSIDERATIONS

2.1 Reasons for Study

The use of all-movable controls on missiles for trim and maneuvering is quite common since the greatest effectiveness is very often obtained by using all of the fin area. Since missiles operate over a wide Mach number range, the longitudinal center-of-pressure location of the force produced by the fin can vary substantially. This variation can be increased, further, by the requirement of high angle of attack operation for greater maneuverability and, thus, the requirement for larger control deflection angles. At the higher angles of attack and control deflection angles, nonlinearities are introduced which make the prediction of the center-of-pressure location very difficult. The accurate prediction of this location over the range of flight conditions is important since this location relative to the control hinge-line position affects the hinge moment acting on the fin and this, in turn, affects the capabilities required of the control actuators. Greater capabilities increase the weight of the actuators and their power supplies. In order to minimize this weight, it is important that an optimum fin planform and airfoil section be selected, in addition to the control hinge-line location, so that the hinge moment is kept to a minimum over the range of flight conditions expected.

Until recently preliminary design methods have been available only for the linear range of angle of attack and control deflection for predicting control normal force and hinge moments. In Reference 1 a method was presented for estimating control hinge moments to large angles of attack and control deflections. It was found there that the predictions, at supersonic speeds, were quite accurate as long as strong nose vortex effects were not

present and the forward fins were not producing strong interference effects on the rearward fins. At transonic speeds, all predictions were inaccurate. As a result of this work, the present investigation was undertaken with the goal of developing a method for determining the optimum fin planform, airfoil section, and hinge-line location for a single set of cruciform fins on a body of revolution at supersonic speeds.

2.2 Optimization Factors

A number of factors may affect the determination of the optimum fin planform and airfoil section. One of these is the range of flight conditions which the missile will encounter during its trajectory. These conditions are:

Mach number, M_∞
Dynamic pressure, q_∞
Combined angle of attack, α_c
Roll angle, ϕ
Fin deflection angle, δ

The complete range of these parameters should be investigated since they each individually and in combination affect the fin hinge moment.

Another factor which may influence the selection of the optimum fin is the force which the fin produces. This force must be sufficient to give the missile adequate trim and maneuverability. Thus, certain fins may be ruled out because they do not produce sufficient control.

A factor which could reduce the number of fin planforms which can be considered would be a restriction on fin span. Because of the way the missile is carried or launched, a maximum span restriction may be imposed. There may also be restrictions applied to fin taper ratio or thickness for structural reasons.

The above are some of the factors which may restrict the ranges of some of the variables which must be considered in an optimization study. In the present work and computer program the

fins are restricted to unswept trailing edges and the planform is characterized by

Fin exposed semispan, $(s - a)$

Fin root chord, c_r

Fin taper ratio, $\lambda = c_t/c_r$

From these, the aspect ratio and fin area are determined.

$$\text{Fin aspect ratio, } AR = \frac{4(s - a)}{c_r(1 + \lambda)}$$

$$\text{Fin area, } S_F = \frac{c_r}{2}(1 + \lambda)(s - a)$$

The fin aspect ratio is defined to be that of the fin and its mirror image joined together at their root chords. Three of the above five parameters must be specified and varied in the optimization study. The fin airfoil section assumed in the computer program is shown in the following sketch.

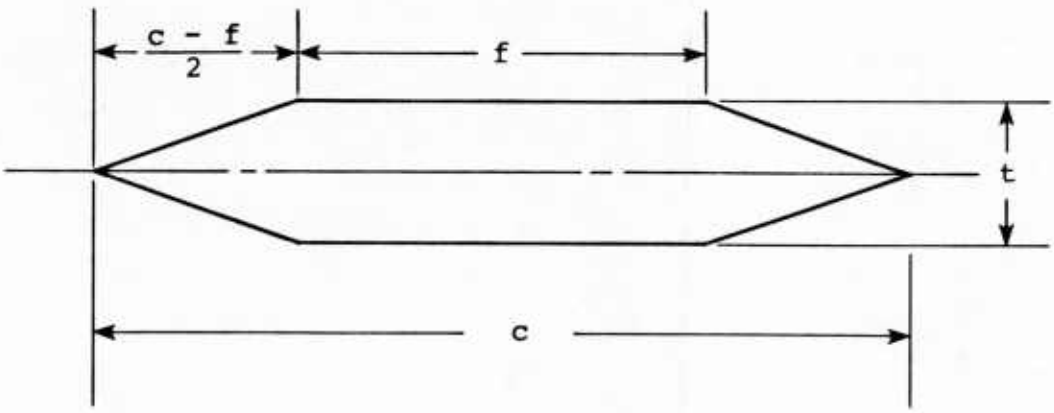

In sections parallel to the root chord, it is assumed to be similar across the span of the fin and consists of a flat plate of length f with equal length wedges for the leading and trailing edges. For the purpose of an optimization study, it is characterized by two parameters.

Thickness to chord ratio, t/c

Flat section to chord ratio, f/c

There are, thus, five fin parameters, three for the planform and two for the airfoil section, which must be varied.

2.3 Use of Program MISSILE2

The computer program MISSILE2, Reference 3, is an engineering prediction method for determining the forces and moments on cruciform missiles to high angles of attack. It predicts fin normal force quite accurately but does not predict the fin axial center-of-pressure location with sufficient accuracy to give a good hinge-moment prediction. In the work of Reference 1, MISSILE2 was modified in order to improve the center-of-pressure prediction and, hence, the hinge moment. The modifications made were

1. Provide accurate wing-alone normal force and center-of-pressure positions as a function of angle of attack as input.
2. Add the capability for determining the effect of free vortices on fin axial center-of-pressure position.
3. Add a better means for extrapolation outside the $AR = 2$ limit of the data base of MISSILE2.
4. Add a better means of extrapolation above $M_\infty = 3$ in the data base.
5. Change the method of accounting for fin-fin interference.

All of these modifications are described in section 4 of Reference 1. With the exception of modification 1, they have all been retained in the present program. Under modification 1, the wing-alone normal-force coefficient and center-of-pressure location were tabular input to the computer program. The present version uses the wing-alone data base contained in MISSILE2 to determine the wing-alone normal-force coefficient. MISSILE2 has been modified to calculate the wing-alone center-of-pressure location including thickness effects as a function of angle of attack therefore eliminating that as input data. The methods used are described

in section 4.2 of Reference 1. Some other modifications have also been made. All modifications will be described in the next section.

3. MODIFICATIONS TO PROGRAM MISSILE2

A number of modifications have been made to program MISSILE2 since the work described in Reference 1. They are

1. Specification of the fin airfoil section as input data
2. Calculation of the flat-plate axial center-of-pressure location for the fin (no thickness effects)
3. Calculation of the axial center-of-pressure shift due to fin thickness distribution.
4. Determination of fin axial center-of-pressure location at high angles of attack
5. Tabulation of maximum and minimum hinge moments as a function of Mach number and hinge-line location

In the following sections, the above items and their implementation in the computer program will be described. A full description of MISSILE2 will not be given since this information is contained in References 2 and 3. Similarly, the modifications made during the work of Reference 1 will not be described since that reference contains a complete description.

3.1 Airfoil Section Specification

The fin airfoil section is used in determining the axial center-of-pressure shift due to fin thickness. This calculation requires knowledge of the local surface slope of the airfoil as a function of distance along the chord at a series of locations across the span of the fin. In the modification presently in the computer program the assumptions have been made that the airfoil section is a flat plate with equal wedge angles in the streamwise direction for the leading and trailing edges and

that the airfoil sections are similar across the span of the fin. The airfoil section is shown in Figure 1 and is defined by two parameters; the thickness to chord ratio, t/c, and the flat-plate length to chord ratio, f/c. These two quantities are input to the computer program as is the number of strips across the span of the fin to be used in the strip-theory calculation of the center-of-pressure shift due to thickness.

3.2 Axial Center-of-Pressure Location Without Thickness Correction

The axial center-of-pressure location for a fin with no thickness is determined using linear theory. This quantity, for most planforms, can be obtained from figure 4.1.4.2-26 of DATCOM, Reference 4. For delta wings the center of pressure is always at the 2/3 root-chord location. For rectangular wings with effective aspect ratios, βAR, equal to or greater than one

$$\left(\frac{\bar{x}}{c_r}\right)_{nt} = \frac{1}{2}\left[\frac{1 - 2/(3\beta AR)}{1 - 1/(2\beta AR)}\right] \qquad (1)$$

where $\beta = \sqrt{M_\infty^2 - 1}$ and the aspect ratio, AR, is that of two fins joined together at their root chords. If βAR is less than one, $\bar{x}/c_r$ is obtained from the following table which was obtained from Chart 10 of Reference 5.

βAR	$\left(\bar{x}/c_r\right)_{nt}$
0	0
0.5	0.2
1.0	0.333

The determination of the center of pressure for the fin with no thickness using the above sources of information is automated in the computer program. For delta wings, $\lambda = 0$, $(\bar{x}/c_r)_{nt} = 0.667$. For a rectangular wing, $\lambda = 1$, equation (1) is used for $\beta AR \geq 1$ and the above table is used for $\beta AR < 1$. A table of values of $(\bar{x}/c_r)_{nt}$ for intermediate values of the taper ratio, λ, obtained from DATCOM for the case of no trailing-edge sweep is included in the

program. Linear interpolation in λ is used to obtain the value of $(\bar{x}/c_r)_{nt}$ for a particular fin. The values obtained from DATCOM are listed in table 1. The quantity $\tan\Lambda_{LE}$ is the tangent of the leading-edge sweep angle of the fin. If $\beta/\tan\Lambda_{LE}$ is less than 1.0, the fin leading edge is subsonic.

3.3 Axial Center-of-Pressure Thickness Correction

The thickness distribution of a fin causes a forward shift from the linear theory value in the axial center-of-pressure position which, as was shown in Reference 1, can be significant. For the cases examined there, shifts which were as much as 15 percent of the root chord were found. See figures 24 through 33 of Reference 1. Thus, if an accurate prediction of fin hinge moment is to be made, this thickness caused shift must be accounted for. If the leading-edge shock wave, in a plane normal to the fin planform and parallel to the root chord, is attached, a strip-theory method using shock-expansion theory is used to calculate the center-of-pressure shift. No method exists for accurately calculating the shift when the leading-edge shock wave is detached. A method which will yield a result, even though it is not valid for this case, is a strip-theory method using Busemann second-order theory. This method has been used in the present computer program. The methods for the attached and detached shock-wave cases will now be described.

3.3.1 Shock-expansion theory for attached shock waves.- For the attached shock-wave case, strip theory is used to calculate the fin axial center-of-pressure shift due to fin thickness. In this method the fin is divided into a series of strips across the span of the fin and the center-of-pressure shift using shock-expansion theory is calculated for each strip. The shifts for the various strips are integrated spanwise across the fin to determine the shift for the complete fin. The details of the method will not be presented in this report since they are contained in section 4.2.2 and Appendix B of Reference 1.

All of the above has been added to the computer program. The method as programmed is restricted to the family of airfoils described in section 3.1 of this report. The method, itself, is valid for a fin planform composed of any number of straight-line segments and a varying airfoil section across the span of the fin. The computer program starts at an angle of attack of 2 degrees and calculates the center-of-pressure shift due to thickness, $(\Delta\bar{x}/c_r)_t$, up to the angle of attack approximately equal to that for shock detachment.

3.3.2 Busemann theory for detached shock wave.- For the detached shock-wave case, strip theory is also used to calculate the fin axial center-of-pressure shift due to fin thickness. The difference between this case and the attached shock case is that Busemann second-order theory is used to calculate the airfoil-section pressure distribution rather than shock-expansion theory. Busemann theory does not apply to the detached shock-wave case but, as will be seen, it does exhibit the correct behavior relative to center-of-pressure values where the shock wave is attached. In lieu of a better method, it is used in the present computer program but the results should probably be used cautiously.

The Busemann theory pressure distribution is calculated using the following equations which are taken from page 243 of Reference 6.

$$\left.\begin{aligned} C_{P_{\ell_i}} &= C_1(\alpha + \theta_i) + C_2(\alpha + \theta_i)^2 \\ C_{P_{u_i}} &= -C_1(\alpha - \theta_i) + C_2(\alpha - \theta_i)^2 \end{aligned}\right\} \tag{2}$$

where

$$\left.\begin{aligned} C_1 &= \frac{2}{\sqrt{M_\infty^2 - 1}} \\ C_2 &= \frac{(\gamma + 1)M_\infty^4 - 4(M_\infty^2 - 1)}{2(M_\infty^2 - 1)^2} \end{aligned}\right\} \tag{3}$$

In the above equations

α = fin angle of attack (see fig. 1)

θ_i = slope of the i*th* region of the airfoil section (see fig. 1)

M_∞ = free-stream Mach number

γ = ratio of specific heats, $\gamma = 1.4$ for air

The subscript i refers to the i*th* region of the airfoil section as described in Appendix B of Reference 1. Equations (2) and (3), above, replace the equations presented in section B.1 of that Appendix for calculating the airfoil-section pressure distribution. This method is incorporated in the computer program for calculating the center-of-pressure shift due to fin thickness. The calculation is only done for $\alpha = 2°$ since the Busemann theory does not apply to the detached shock case. This value is added to the nonthickness center of pressure, $(\bar{x}/c_r)_{nt}$, and linear interpolation between the resulting value and the $\alpha = 45°$ value, obtained as described in the following section, is used to obtain the center of pressure at other angles of attack.

To show how the center-of-pressure location for a Mach number where the shock wave is detached fairs into the values where it is attached, calculations were made for the fin shown in figure 2. The results are shown in figure 3. The quantity $\bar{x}/c_r$ is

$$\frac{\bar{x}}{c_r} = \left(\frac{\bar{x}}{c_r}\right)_{nt} - \left(\frac{\Delta\bar{x}}{c_r}\right)_t \tag{4}$$

For $M_\infty = 1.2$ and 1.3 the shock wave is detached and for the other Mach numbers it is attached. Going from $M_\infty = 1.6$ to $M_\infty = 1.2$ there is a forward movement of the center of pressure. If the experimental data shown in figures 15 through 18 of Reference 1 are examined, the same trend is observed. Thus, the Busemann theory, even though not strictly applicable to a detached shock case, produces a center-of-pressure shift in the correct direction.

3.4 Axial Center-of-Pressure Location for an Angle of Attack of 45°

Sections 3.2 and 3.3 present methods for predicting the fin-alone center-of-pressure location as a function of angle of attack up to the angle at which shock detachment occurs. If the shock is detached at $\alpha = 2°$ a method is presented for estimating the center-of-pressure location at this angle. Knowledge of the value of $\bar{x}/c_r$ for the fin at some large angle, like 45° where $\bar{x}/c_r$ tends toward the centroid of area, would allow the low angle values to be faired to this value. In this way an estimate of $\bar{x}/c_r$ over a large angle range could be made.

To obtain values of $\bar{x}/c_r$ at $\alpha = 45°$ for a range of Mach numbers, M_∞, aspect ratios, $\mathcal{R}$, and taper ratios, λ, the wing-alone data base of Reference 7 has been utilized. These data are plotted in figure 4 along with data from the data base of Reference 8. Curves have been faired through the Reference 7 data. This set was chosen since the data of Reference 8 were obtained on a semi-span model mounted on a reflection plane and may be affected by boundary-layer separation at large angles of attack. Values of $\bar{x}/c_r$ have been read from the faired curves and are tabulated in table 2. These data have been incorporated into the computer program as a data base. Triple linear interpolation is performed in the data to obtain $\bar{x}/c_r$ at $\alpha = 45°$ for a given M_∞, $\mathcal{R}$, and λ. If the value of $\mathcal{R}$ is greater than 2.0, linear extrapolation in $\mathcal{R}$ is used.

3.5 Center-of-Pressure Calculation Procedure

For a given Mach number, the computer program calculates a table of $\bar{x}/c_r$ versus α using the methods described in the previous three sections, sections 3.2 through 3.4. The first step in this calculation is to use the method of section 3.2 to calculate the fin alone center-of-pressure position for the given values of M_∞, $\mathcal{R}$, and λ. This provides the value of $(\bar{x}/c_r)_{nt}$, the center of pressure without thickness effects. The thickness correction,

$(\Delta x/c_r)_t$, is next calculated as a function of α for the same value of M_∞, the input airfoil section, and the fin planform. This calculation is made using the procedures described in section 3.3 up to the shock-wave detachment angle. The center of pressure of the fin alone as a function of α is then determined using Equation (4). A table of $\bar{x}/c_r$ for angles of attack up to the leading-edge shock-wave detachment angle has now been determined. The last entry in the table is next calculated for $\alpha = 45°$ using the method in section 3.4.

This table of $\bar{x}/c_r$ versus α is now used to determine the center of pressure of the fin in the presence of the body for the given values of M_∞, ϕ, δ, and α_c. The first step in the program is to calculate the normal-force coefficient of the fin in the presence of the body. This is done using the methods described in References 2 and 3. After this, the fin-alone normal-force data base in the program is entered to find the angle of attack which produces this normal force. Using this angle of attack, the table constructed as described in the preceeding paragraph is entered to determine the value of $\bar{x}/c_r$ corresponding to this angle of attack. This value of $\bar{x}/c_r$ is used in the hinge-moment coefficient calculation.

3.6 Maximum and Minimum Hinge Moment Tabulation

In order to determine an optimum fin planform and airfoil section which minimizes fin hinge moment, calculations must be made for a large number of different fins over the complete range of flight conditions to be encountered, that is, Mach number, angle of attack, and fin deflection angle. Program MISSILE2 as used in References 1 and 3 only allows one Mach number and one fin deflection angle per case so that many cases would have to be run to examine the hinge moment for all flight conditions (combinations of M_∞, ϕ, α_c, and δ). To alleviate this, the program has been modified to allow a series of values of M_∞ and δ to be run in the same case.

The program has also been changed so that the maximum and minimum hinge moments are summarized in a table. A sample of this table is shown in figure 5. For a given roll angle, the maximum and minimum hinge moments are tabulated as a function of Mach number, M_∞, and hinge-line location x_{HL}/c_r, for fin 4. Fin 4 is the right horizontal fin viewed from the rear with the configuration at zero degrees roll. The direction of positive hinge moment, C_{HM}, is shown in figure 6. The values tabulated in figure 5 are determined by calculating C_{HM} for all α_c, δ combinations for a given x_{HL} and M_∞. This table of values is then searched to find the maximum and minimum values.

4. DETERMINATION OF OPTIMUM HINGE-LINE LOCATION FOR A PARTICULAR FIN

The optimum hinge-line location is the point along the fin root chord where the magnitudes of the maximum and minimum hinge-moment coefficients reach a minimum value when they are considered together. To illustrate how this is determined, the table of values in figure 5 will be used. This table was discussed in section 3.6. The body-canard combination for which the calculation was made is shown in figure 7 and the fin details in figure 2. The flight conditions used were

$$M_\infty = 1.2,\ 1.6,\ 2.0,\ 2.5,\ 3.0$$

$$\phi = 0°$$

$$\delta_{1,3} = 0°$$

$$\delta_{2,4} = -20°,\ -10°,\ 0°,\ 10°,\ 20°$$

$$\alpha_c = 0°,\ 5°,\ 10°,\ 15°,\ 20°$$

This is a total of 125 points.

Scanning down the table we see that both the maximum and minimum hinge moments reach a minimum magnitude at x_{HL}/c_r of 0.63 or 0.64. The hinge moments in this region will be plotted. To determine the points to plot, the maximum magnitude for the five

Mach numbers for which calculations were made is selected. These values are underlined in the table from $x_{HL}/c_r = 0.60$ to 0.67 and are plotted in figure 8. The optimum hinge-line location is the point at which the two curves intersect, $x_{HL}/c_r = 0.6322$. If the hinge line is located at this point, the maximum magnitude of the hinge moment for the above flight conditions will not exceed $|C_{HM}| = 0.015$. Sometimes the two curves exhibit the behavior shown in the following sketch. In this case the optimum location

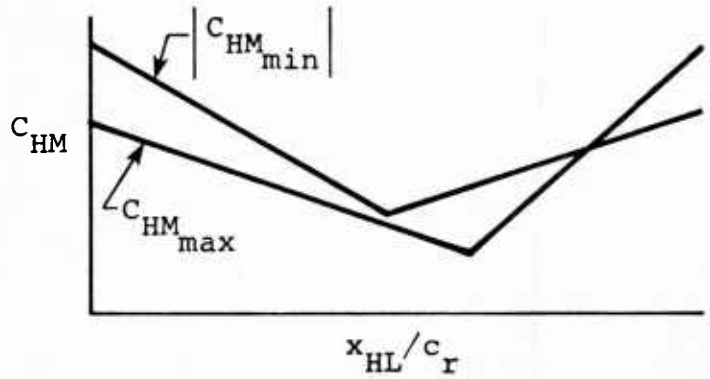

of the hinge line is not where the two curves intersect but at the point where the upper curve reaches a minimum.

The above procedure has been used in obtaining all of the results to be presented in section 5.

5. DETERMINATION OF OPTIMUM FIN TO MINIMIZE HINGE-MOMENT COEFFICIENT

The method which has been described will now be used to determine the planform and the airfoil section of a fin which will minimize the magnitude of the fin hinge-moment coefficient. The configuration used is the body shown in figure 7 with various fins. The leading edge of the root chord of all fins is at the location shown in this figure. The body extends to the fin trailing edge. Since the fin root chord will vary in length, the body length will vary from that shown in the figure.

For all of the calculations to be shown, the flight condition envelope is the same as that used in section 4. That is

$$M_\infty = 1.2,\ 1.6,\ 2.0,\ 2.5,\ 3.0$$

$$\phi = 0°$$

$$\delta_{1,3} = 0°$$

$$\delta_{2,4} = -20°,\ -10°,\ 0°,\ 10°,\ 20°$$

$$\alpha_c = 0°,\ 5°,\ 10°,\ 15°,\ 20°$$

The roll angle, ϕ, is not varied since experimental data show that the maximum hinge moment acting on a canard fin occurs very close to $\phi = 0°$, fin horizontal, and is almost equal to the value at $\phi = 0°$. This is shown in figures 84 through 89 of Reference 1. If strong body-vortex effects are present this may not be the case and ϕ must be varied. The same is true when forward fins induce large effects on rear fins. The value of ϕ can be varied in the computer program if desired.

The following parameters are available for specifying the fin planform.

Aspect ration, AR
Fin area, S_F
Fin taper ratio, λ
Fin root-chord length, c_r
Exposed semispan of fin, $(s - a)$

In the results to be presented, the value of S_F will be held constant at 14.0625 in^2. Two aspect ratios will be considered, AR = 2.0 and 3.0. The optimization will, thus, be done for two different aspect ratio fins with the same area. The equation for the aspect ratio is

$$AR = \frac{4(s - a)}{c_r(1 + \lambda)} \tag{5}$$

where the aspect ratio is that of two fins joined together at their root chords. The fin area is

$$S_F = \frac{c_r}{2}(1 + \lambda)(s - a) \tag{6}$$

From these two equations

$$(s - a) = \sqrt{\frac{S_F \text{AR}}{2}} \tag{7}$$

and

$$c_r = \frac{2S_F}{(s - a)(1 + \lambda)} \tag{8}$$

Two parameters specify the airfoil section

Thickness to chord ratio, t/c
Flat-section length to chord ratio, f/c

For all of the results, the reference area is taken to be the cross-sectional area of the cylindrical section of the body, $S_R = 19.635$ in^2, and the reference length is the body diameter, d = 5 in. These are used in forming all force and moment coefficients.

The order of optimization used is taper ratio, airfoil section, body-radius to fin-span ratio, and, finally, aspect ratio. These will now be discussed in order.

5.1 Taper-Ratio Optimization

For the taper ratio optimization study, the fin airfoil section for both AR = 2.0 and 3.0 was held constant with

$$t/c = 0.06$$
$$f/c = 0.25$$

The quantity (s - a) is a function of aspect ratio and fin area [Eq. (7)] so that for the two aspect ratios

$$a/s = 0.4 \; ; \quad \text{AR} = 2.0$$
$$a/s = 0.3525 \; ; \quad \text{AR} = 3.0$$

The value of the magnitude of the maximum hinge moment with the hinge line in the optimum position is shown in figure 9 as a function of fin taper ratio. For both aspect ratios, the lowest hinge moment occurs for a fin of delta planform, $\lambda = 0$. As a result, a delta planform is determined to provide the minimum

magnitude hinge moment over the envelope of flight conditions. A value of $\lambda = 0$ will be used in the following steps of the optimization.

5.2 Airfoil-Section Optimization

The results of the airfoil section optimization study are shown in figure 10 for the optimum taper ratio of $\lambda = 0$. In this figure the value of $|C_{HM_{opt}}|$ is plotted against thickness ratio, t/c, for various values of the flat plate parameter, f/c. For both aspect ratios, the same behavior is observed. The minimum value of $|C_{HM_{opt}}|$ is fairly insensitive to f/c and, as this parameter increases in value, the minimum value occurs at smaller values of t/c. For both aspect ratios, the double-wedge airfoil, f/c = 0, is nearly the optimum one. As a result of this study, the following airfoil-section parameters were chosen for the two aspect ratios. They are very near the optimum values.

AR = 2.0, t/c = 0.06, f/c = 0.5

AR = 3.0, t/c = 0.05, f/c = 0.5

5.3 Body-Radius to Fin-Span Ratio Optimization

For a taper-ratio zero fin and using the above airfoil-section quantities, calculations were made varying the body-radius to fin-span ratio, a/s. The results of these calculations showed that the value of $|C_{HM_{opt}}|$ did not vary with a/s.

5.4 Aspect-Ratio Optimization

Results have been presented in the preceeding sections for values of the aspect ratio of 2.0 and 3.0. Figure 10 shows that the minimum value of $|C_{HM_{opt}}|$ increases with increasing aspect ratio. This is probably to be expected since the normal force at a given angle of attack increases with aspect ratio, everything else being held constant. This could be verified by repeating the above calculations for other aspect ratios. The normal-force coefficients for the two fins are presented in the next section. For these minimum hinge-moment fins, control is still maintained.

5.5 Results for Optimum Fins

The previous sections have taken two fins with the same area, $S_F = 14.0625$ in^2, and different aspect ratios and determined the values of the other fin parameters which specify the planform, airfoil section, and hinge-line location to minimize the magnitude of the fin hinge-moment coefficient over the range of assumed flight conditions. The two fins selected are

Quantity	Fin 1	Fin 2
S_F, in^2	14.0625	14.0625
AR	2.0	3.0
λ	0.0	0.0
t/c	0.06	0.05
f/c	0.5	0.5
a/s	0.4	0.3525
x_{HL}/c_r	0.6215	0.6322

The computer program was run in order to examine the hinge-moment and normal-force coefficient variation over the range of M_∞, δ, and α_c with $\phi = 0°$. The results of these calculations are shown in figure 11. Hinge-moment coefficient, C_{HM}, is plotted versus normal-force coefficient, C_{NF}. The curves are for the various free-stream Mach numbers.

The results for the AR = 2.0 fin are shown in figure 11(a). The $M_\infty = 1.2$ curve has symbols showing the results for the five values of α_c for the five fin deflection angles. As can be seen all 25 points lie on the same curve. Use of the equivalent angle of attack concept causes this. This concept is described in section 4.4.4 and Appendix C of Reference 1, Appendix C of Reference 3, and Reference 9. To obtain a desired C_{NF} a certain value of C_{HM} is produced which can be done for various combinations of α_c and δ. For all combinations of α_c and δ, the normal-force carryover onto the body is the same. Since the nose normal

force increases with increasing α_c, the α_c, δ combination with the largest α_c should be used for the best maneuverability.

As can be seen, the center of pressure for $M_\infty = 1.2$ is ahead of the hinge line while that for the other values of M_∞ is behind the hinge line. This behavior is consistent with experimental data which show a forward shift in the center of pressure in the transonic speed range. For this fin the $M_\infty = 1.6$ to 3.0 results are grouped quite close together.

The AR = 3.0 results are shown in figure 11(b). The results are similar to those for AR = 2.0 although there is more of a Mach number effect for $M_\infty = 1.6$ to 3.0. It is of interest to compare the results of the two values of AR. At $M_\infty = 1.2$ the maximum value of C_{NF} is about the same for the two aspect ratios while the maximum magnitude of the hinge-moment coefficient has increased by about 60 percent for the AR = 3.0 fin. At $M_\infty = 3.0$ the maximum normal-force coefficient is about 140 percent higher for AR = 3.0 than at 2.0 while the maximum magnitude of the hinge-moment coefficient has increased by about 50 percent. Thus, at $M_\infty = 1.2$ for a constant area fin, increasing the aspect ratio from 2.0 to 3.0 results in no increase in normal-force coefficient but there is a 60 percent increase in hinge-moment coefficient. At $M_\infty = 3.0$ the increase in aspect ratio produces a 140 percent increase in normal-force coefficient with only a 50 percent increase in hinge-moment coefficient.

6. CONCLUDING REMARKS

This report presents the results of the second phase of a study of the hinge moments of all-movable controls as used on cruciform missiles. In phase one of the study, a predictive method was developed for predicting the hinge moments acting on the controls and the range of applicability of the method was determined. It was found that the method was applicable to the Mach number range of 1.3 to 3.7 except for leeward fins when strong body vortices were present. As a result, phase two, this

phase of the study, was undertaken with the purpose of developing an optimization technique using the computer program which would determine the fin planform, airfoil section, and hinge-line location which would minimize fin hinge-moment coefficient.

As a result of this goal, certain of the calculations done in phase one external to the program have been included in the present computer program. With minimum changes to the input data, the hinge moments produced by an all-movable control over a wide range of flight conditions, fin planform, and fin airfoil section can be studied. The configuration is restricted to a body with one set of cruciform fins.

An optimization procedure is presented which allows the user of the program to determine the optimum fin planform, airfoil section, and hinge-line location to minimize fin hinge-moment coefficient subject to constraints he may apply through the input data to the program. The range of flight conditions to be studied, that is, Mach number, roll angle, angle of attack, and fin deflection angle, are specified as input data. Through input data, the fin planform and airfoil section may also be restricted. In this way trade-off studies can be carried out over the ranges of conditions.

The report presents an example of an optimization study where the fin area is fixed and all other parameters are free to vary for a given range of flight conditions. This example illustrates the use of the program for a study such as this. The computer program and its use is described in an appendix of this report. The range of applicability of the program is

Mach number; 1.2 to 4.0
Roll angle; -90° to 90°
Angle of attack; 0° to 20°
Fin deflection angle; -20° to 20°
Aspect ratio; 0.5 to 4.0
Taper ratio; 0.0 to 1.0

The fin airfoil section is restricted to a flat plate with equal length wedges for the leading and trailing edges. This is not a restriction on the method but one imposed by the program.

As a result of the optimization study presented in this report, the following conclusions can be drawn.

1. Hinge-line location was the most important parameter in minimizing $|C_{HM_{opt}}|$.
2. Fin taper ratio had a large effect with the smallest $|C_{HM_{opt}}|$ occurring at low values of λ (0 to 0.25).
3. The value of $|C_{HM_{opt}}|$ was insensitive to body-radius to fin-span ratio.
4. The minimum value of $|C_{HM_{opt}}|$ was quite insensitive to various combinations of t/c and f/c. However, if a given value of t/c must be used for structural reasons, the right value of f/c must be selected.
5. Increasing the aspect ratio from 2.0 to 3.0 caused an increase in the minimum $|C_{HM_{opt}}|$ of 50 to 60 percent. At $M_\infty = 1.2$ the maximum C_{NF} was not changed whereas at $M_\infty = 3.0$ it was increased about 140 percent.

The present work used one optimization scenario, that of minimizing the maximum value of $|C_{HM}|$ for a constant area fin. The computer program can be easily changed to handle other scenarios.

REFERENCES

1. Nielsen, J. N. and Goodwin, F. K.: Preliminary Method for Estimating Hinge Moments of All-Movable Controls. NEAR TR 268, Mar. 1982.

2. Nielsen, J. N., Hemsch, M. J., and Smith, C. A.: A Preliminary Method for Calculating the Aerodynamic Characteristics of Cruciform Missiles to High Angles of Attack Including Effects of Roll Angle and Control Deflections. Report ONR-CR215-226-4F, Nov. 1977.

3. Smith, C. A. and Nielsen, J. N.: Prediction of Aerodynamic Characteristics of Cruciform Missiles to High Angles of Attack Utilizing a Distributed Vortex Wake. NEAR TR 208, Jan. 1980.

4. McDonnell-Douglas Aircraft Co.: USAF Stability and Control DATCOM. Revised Apr. 1978.

5. Pitts, W. C., Nielsen, J. N., and Kaattari, G. E.: Lift and Center of Pressure of Wing-Body-Tail Combinations at Subsonic, Transonic, and Supersonic Speeds. NACA Report 1307, 1957.

6. Nielsen, J. N.: Missile Aerodynamics, McGraw-Hill Book Co., 1960.

7. Stallings, R. L., Jr. and Lamb, M.: Wing-Alone Aerodynamic Characteristics for High Angles of Attack at Supersonic Speeds. NASA Technical Paper 1889, Jul. 1981.

8. No author listed: High Alpha Aerodynamics – Fin Alone (Data Reported in AEDC-TR-75-124). Vols. 1 and 2, Propulsion Wind Tunnel Facility, ARO, Inc., Jul. 1974.

9. Hemsch, M. J. and Nielsen, J. N.: The Equivalent Angle-of-Attack Method for Estimating the Nonlinear Characteristics of Missile Wings and Control Surfaces. AIAA Paper 82-133. Paper presented at AIAA 9th Atmospheric Flight Mechanics Conference, San Diego, CA, Aug. 9-11, 1982.

Table 1.- Values of $(\bar{x}/c_r)_{nt}$ obtained from DATCOM for $M_\infty > 1.0$ for fins with unswept trailing edges.

$\frac{\beta}{\tan\Lambda_{LE}}$	$\left(\bar{x}/c_r\right)_{nt}$			
	$\lambda = .2$	$\lambda = .25$	$\lambda = .33$	$\lambda = .5$
0.0	0.535	0.500	0.450	0.345
0.2	0.575	0.535	0.500	0.386
0.4	0.605	0.565	0.535	0.422
0.6	0.618	0.590	0.557	0.454
0.8	0.625	0.600	0.572	0.483
1.0	0.630	0.605	0.578	0.510

$\frac{\tan\Lambda_{LE}}{\beta}$	$\left(\bar{x}/c_r\right)_{nt}$			
	$\lambda = .2$	$\lambda = .25$	$\lambda = .33$	$\lambda = .5$
0.0	0.650	0.652	0.640	0.612
0.2	0.648	0.652	0.635	0.601
0.4	0.645	0.650	0.627	0.585
0.6	0.640	0.644	0.618	0.563
0.8	0.635	0.630	0.600	0.538
1.0	0.630	0.605	0.578	0.510

Table 2.- Values of $\bar{x}/c_r$ at $\alpha = 45°$ as determined from the Stallings-Lamb data base.

M_∞	AR = 1/2			AR = 1			AR = 2		
	$\lambda = 0$	$\lambda = 1/2$	$\lambda = 1$	$\lambda = 0$	$\lambda = 1/2$	$\lambda = 1$	$\lambda = 0$	$\lambda = 1/2$	$\lambda = 1$
1.0	0.601	0.535	0.435	0.570	0.545	0.430	0.618	0.545	0.417
1.4	0.626	0.551	0.435	0.610	0.555	0.430	0.620	0.546	0.417
1.8	0.638	0.562	0.436	0.629	0.560	0.430	0.621	0.547	0.416
2.2	0.642	0.570	0.437	0.637	0.565	0.429	0.623	0.548	0.415
2.6	0.643	0.574	0.438	0.640	0.565	0.428	0.625	0.549	0.415
3.0	0.644	0.578	0.439	0.640	0.565	0.428	0.627	0.549	0.414
3.8	0.645	0.580	0.440	0.640	0.565	0.427	0.630	0.550	0.413
4.6	0.646	0.580	0.441	0.640	0.565	0.426	0.633	0.551	0.411

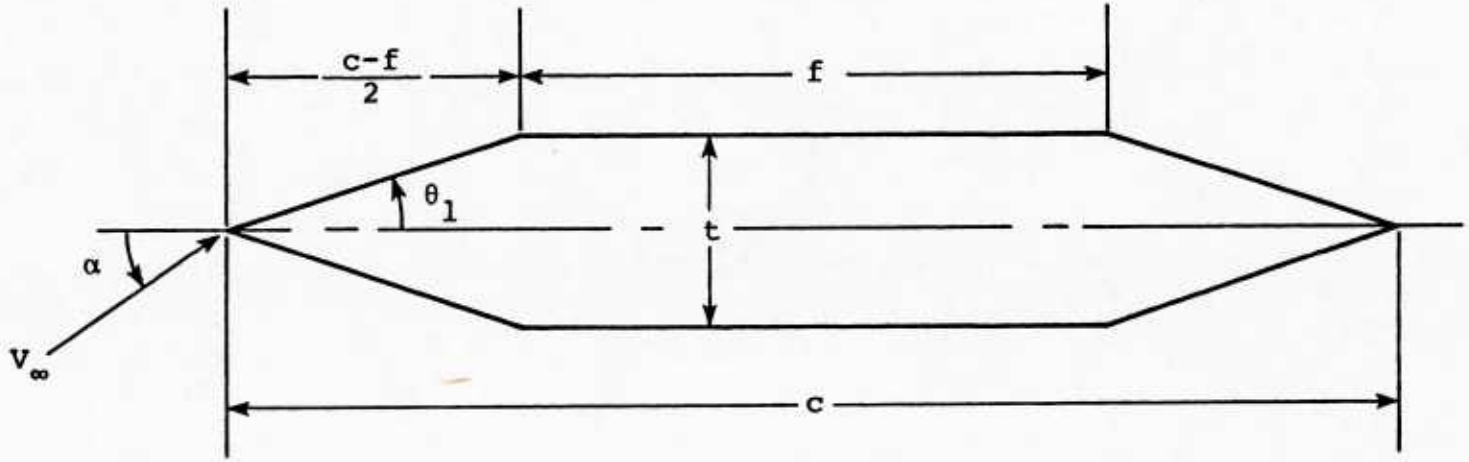

Figure 1.- Airfoil section in computer program.

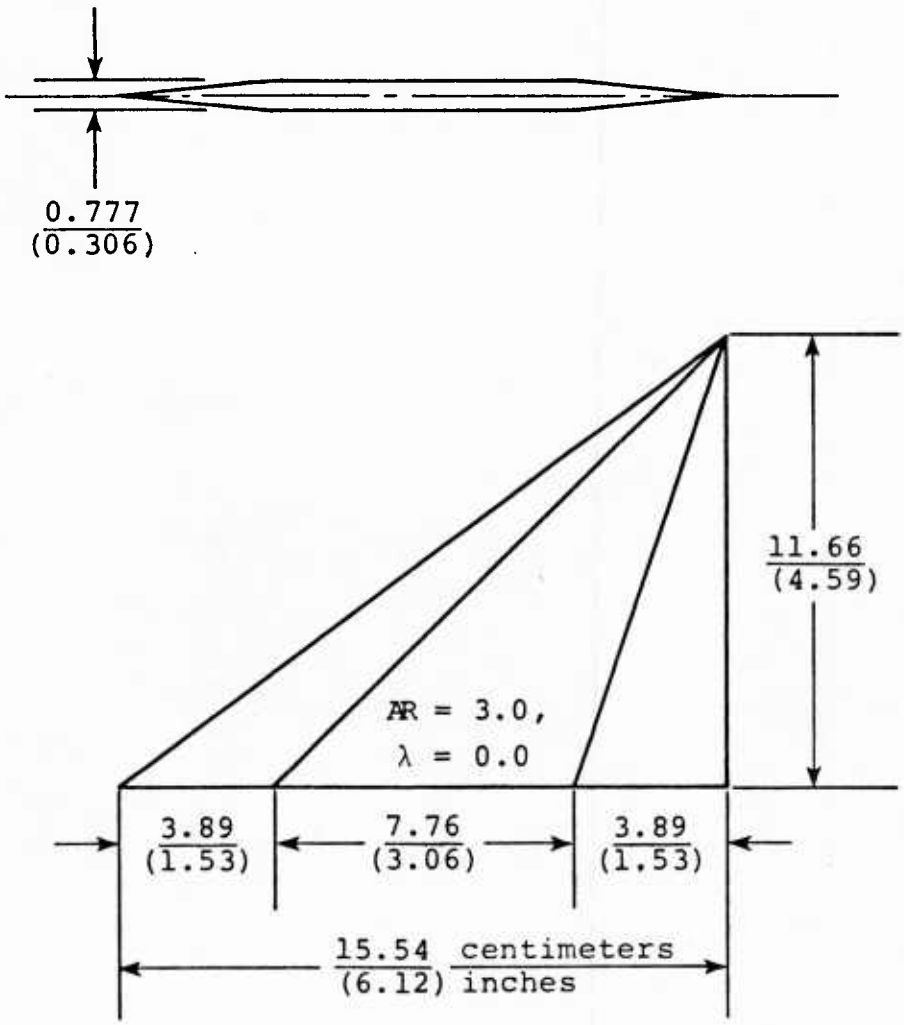

Figure 2.- Dimensions of an AR=3.0, λ=0.0 fin.

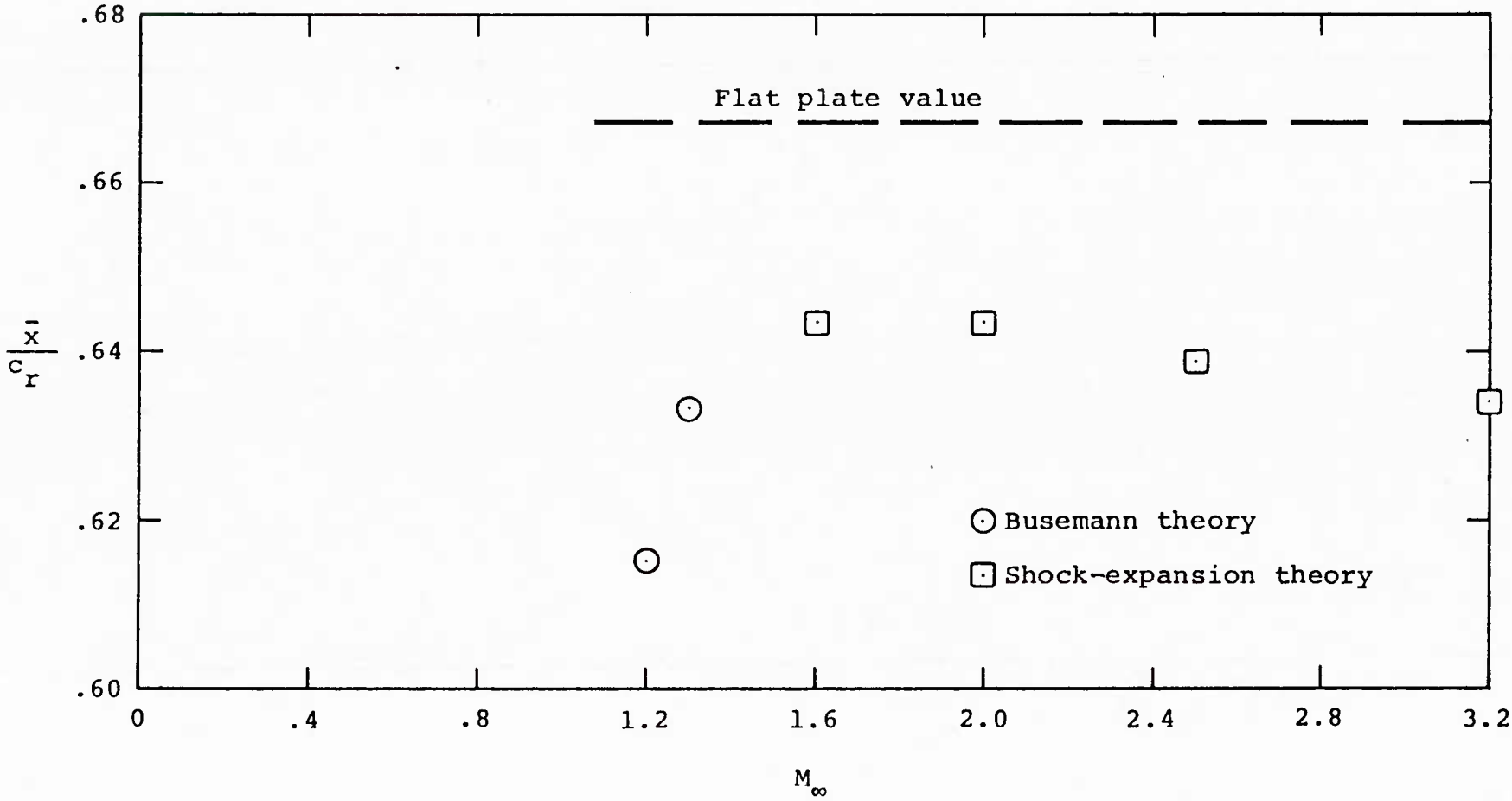

Figure 3.- Center-of-pressure location as a function of Mach number for an AR = 3.0, λ = 0.0 fin.

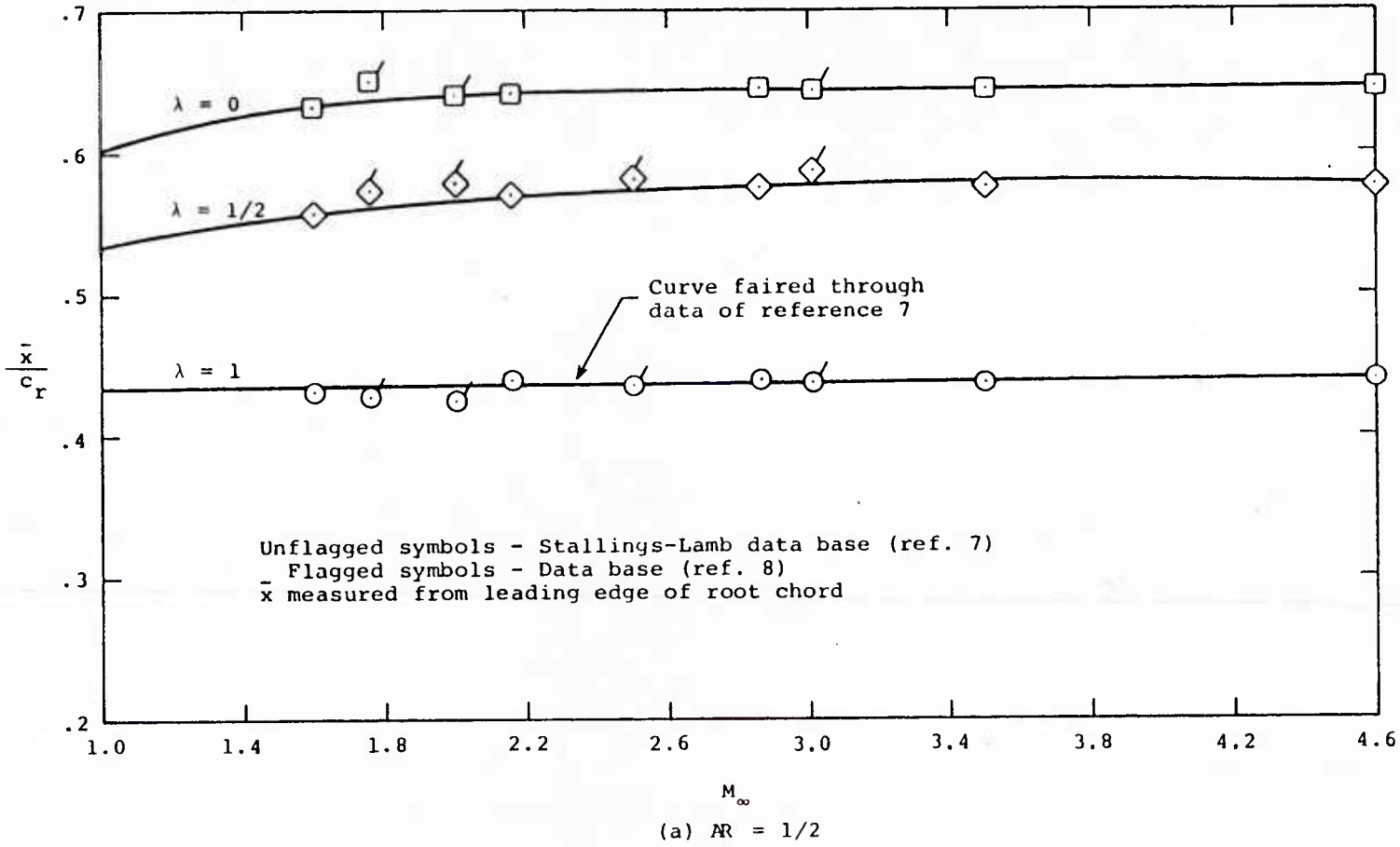

(a) AR = 1/2

Figure 4.- Comparison of axial center-of-pressure position at $\alpha = 45°$ of the data bases of references 7 and 8.

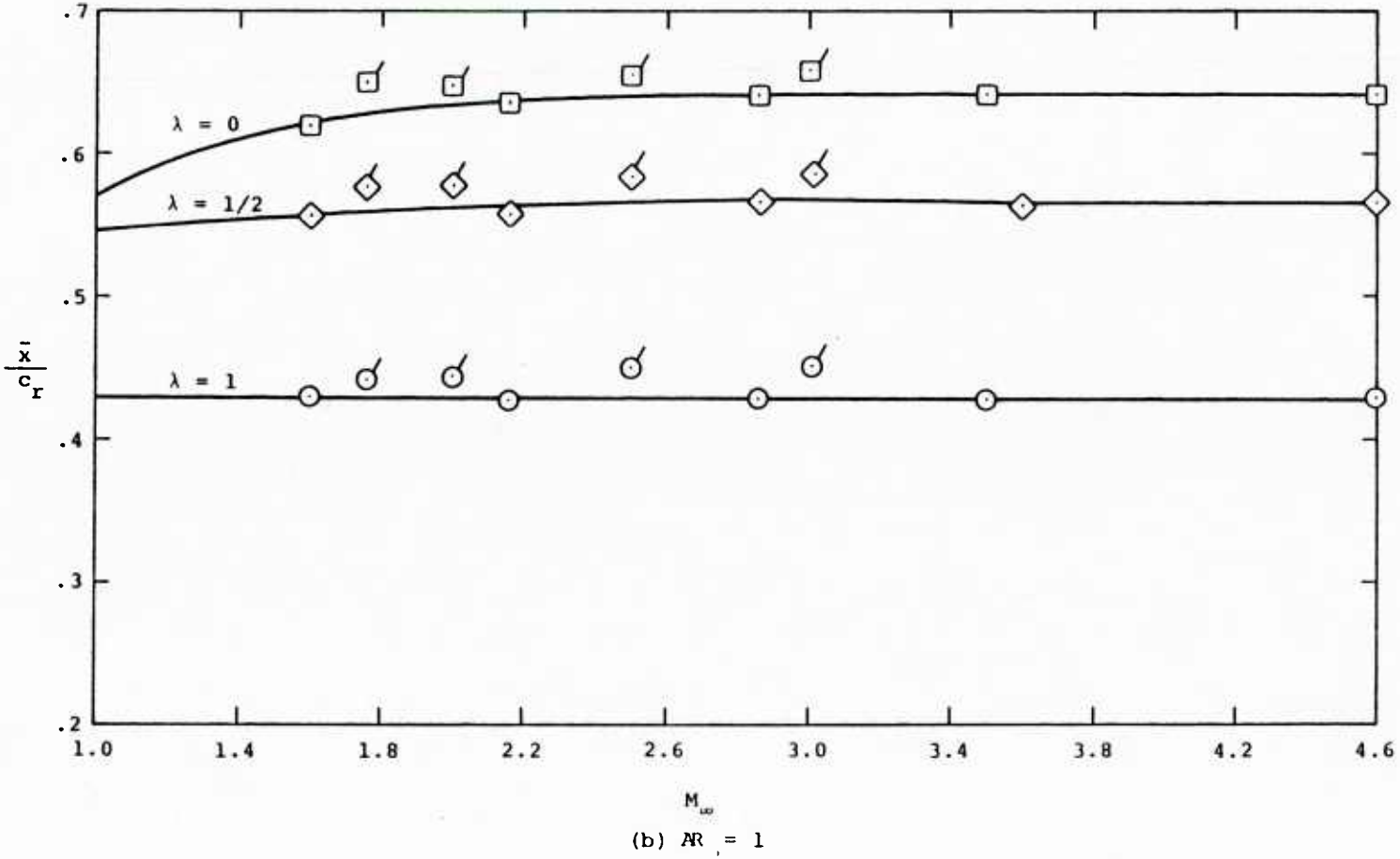

(b) AR = 1

Figure 4.- Continued.

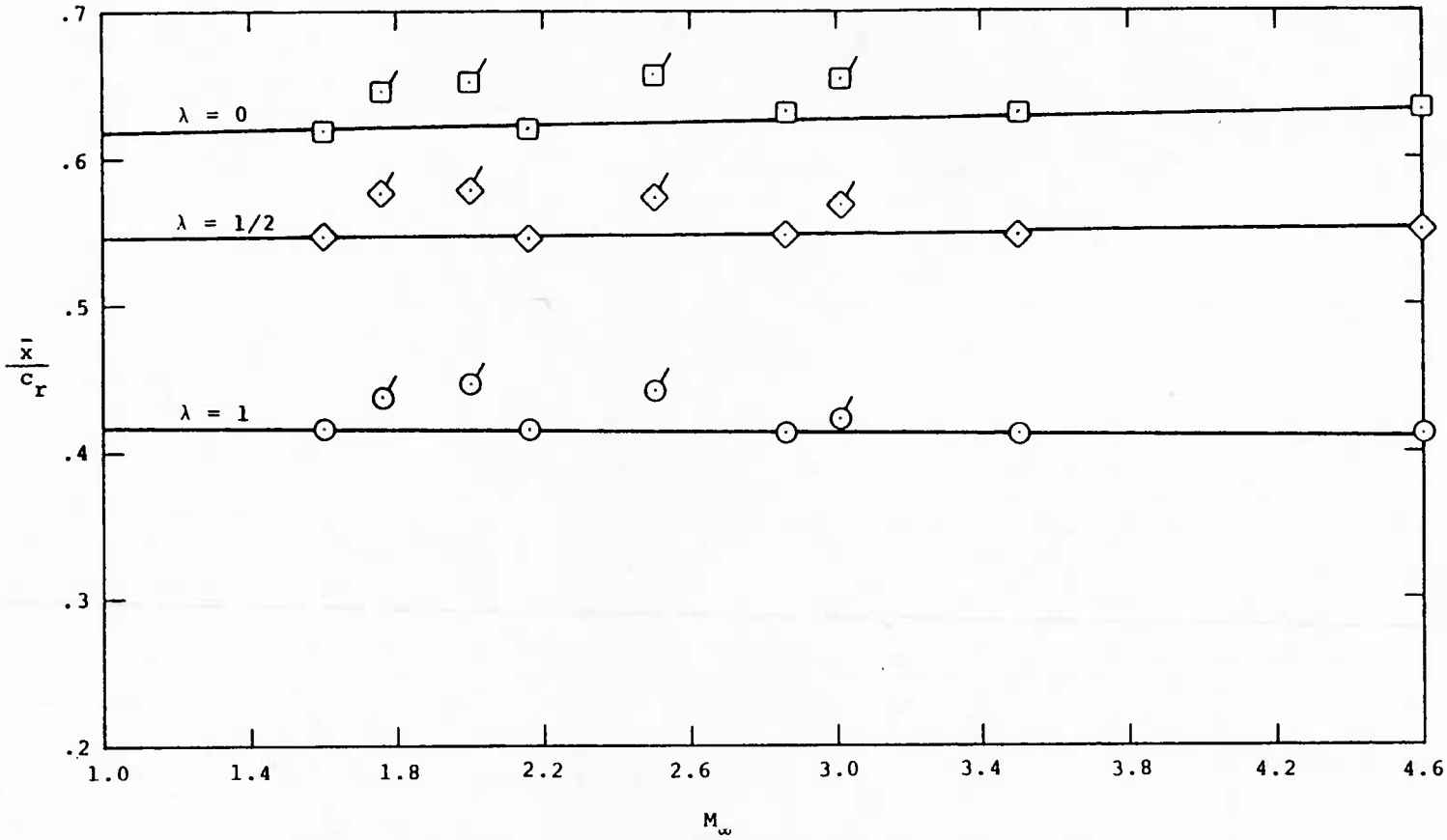

(c) AR = 2

Figure 4.- Concluded.

MAXIMUM AND MINIMUM HINGE MOMENTS FOR FIN 4 (BASED ON SROUT AND LROUT), OVER THE RANGES OF ANGLE OF ATTACK AND FIN DEFLECTION ANGLE FOR WHICH CALCULATIONS WERE MADE, FOR A GIVEN ROLL ANGLE, THEY ARE TABULATED AS A FUNCTION OF HINGE-LINE LOCATION AND MACH NUMBER.

ROLL ANGLE (PHI) = 0.00

•••••••••••••• MAXIMUM HINGE MOMENT ••••••••••••••						•••••••••••••• MINIMUM HINGE MOMENT ••••••••••••••					
XHL/CR	M=1.20	M=1.60	M=2.00	M=2.50	M=3.00	XHL/CR	M=1.20	M=1.60	M=2.00	M=2.50	M=3.00
.20	.3461	.3801	.4078	.4529	.4944	.20	-.5706	-.6246	-.7077	-.8252	-.9436
.21	.3379	.3713	.3984	.4424	.4829	.21	-.5577	-.6099	-.6910	-.8059	-.9219
.22	.3298	.3626	.3890	.4320	.4714	.22	-.5449	-.5953	-.6743	-.7867	-.9003
.23	.3216	.3538	.3796	.4216	.4599	.23	-.5321	-.5806	-.6575	-.7674	-.8786
.24	.3135	.3450	.3702	.4111	.4484	.24	-.5192	-.5659	-.6408	-.7481	-.8570
.25	.3054	.3363	.3608	.4007	.4369	.25	-.5064	-.5513	-.6241	-.7289	-.8353
.26	.2972	.3275	.3515	.3902	.4254	.26	-.4936	-.5366	-.6074	-.7096	-.8137
.27	.2891	.3188	.3421	.3798	.4139	.27	-.4807	-.5219	-.5907	-.6903	-.7920
.28	.2809	.3100	.3327	.3693	.4024	.28	-.4679	-.5073	-.5739	-.6711	-.7704
.29	.2728	.3012	.3233	.3589	.3909	.29	-.4551	-.4926	-.5572	-.6518	-.7487
.30	.2647	.2925	.3139	.3484	.3793	.30	-.4422	-.4779	-.5405	-.6325	-.7271
.31	.2565	.2837	.3045	.3380	.3678	.31	-.4294	-.4633	-.5238	-.6133	-.7054
.32	.2484	.2749	.2951	.3275	.3563	.32	-.4165	-.4486	-.5071	-.5940	-.6838
.33	.2402	.2662	.2857	.3171	.3448	.33	-.4037	-.4339	-.4903	-.5747	-.6621
.34	.2321	.2574	.2764	.3066	.3333	.34	-.3909	-.4193	-.4736	-.5554	-.6405
.35	.2239	.2486	.2670	.2962	.3218	.35	-.3780	-.4046	-.4569	-.5362	-.6188
.36	.2158	.2399	.2576	.2857	.3103	.36	-.3652	-.3899	-.4402	-.5169	-.5972
.37	.2077	.2311	.2482	.2753	.2988	.37	-.3524	-.3753	-.4235	-.4976	-.5755
.38	.1995	.2224	.2388	.2648	.2873	.38	-.3395	-.3606	-.4067	-.4784	-.5539
.39	.1914	.2136	.2294	.2544	.2758	.39	-.3267	-.3459	-.3900	-.4591	-.5322
.40	.1832	.2048	.2200	.2440	.2643	.40	-.3139	-.3313	-.3733	-.4398	-.5106
.41	.1751	.1961	.2106	.2335	.2528	.41	-.3010	-.3166	-.3566	-.4206	-.4889
.42	.1670	.1873	.2013	.2231	.2413	.42	-.2882	-.3019	-.3399	-.4013	-.4673
.43	.1588	.1785	.1919	.2126	.2298	.43	-.2754	-.2873	-.3231	-.3820	-.4457
.44	.1507	.1698	.1825	.2022	.2182	.44	-.2625	-.2726	-.3064	-.3628	-.4240
.45	.1425	.1610	.1731	.1917	.2067	.45	-.2497	-.2579	-.2897	-.3435	-.4024
.46	.1344	.1522	.1637	.1813	.1952	.46	-.2368	-.2433	-.2730	-.3242	-.3807
.47	.1263	.1435	.1543	.1708	.1837	.47	-.2240	-.2286	-.2563	-.3050	-.3591
.48	.1181	.1347	.1449	.1604	.1722	.48	-.2112	-.2139	-.2395	-.2857	-.3374
.49	.1100	.1260	.1356	.1499	.1607	.49	-.1983	-.1993	-.2228	-.2664	-.3158
.50	.1018	.1172	.1262	.1395	.1492	.50	-.1855	-.1846	-.2061	-.2471	-.2941
.51	.0937	.1084	.1168	.1290	.1377	.51	-.1727	-.1699	-.1894	-.2279	-.2725
.52	.0856	.0997	.1074	.1186	.1262	.52	-.1598	-.1553	-.1727	-.2086	-.2508
.53	.0774	.0909	.0980	.1081	.1147	.53	-.1470	-.1406	-.1559	-.1893	-.2292
.54	.0693	.0821	.0886	.0977	.1032	.54	-.1342	-.1259	-.1392	-.1701	-.2075
.55	.0611	.0734	.0792	.0873	.0917	.55	-.1213	-.1113	-.1225	-.1508	-.1859
.56	.0530	.0646	.0698	.0768	.0802	.56	-.1085	-.0966	-.1058	-.1315	-.1642
.57	.0449	.0558	.0605	.0664	.0687	.57	-.0956	-.0819	-.0891	-.1123	-.1426
.58	.0367	.0471	.0511	.0559	.0571	.58	-.0828	-.0673	-.0734	-.0943	-.1209
.59	.0286	.0383	.0417	.0455	.0456	.59	-.0700	-.0526	-.0577	-.0763	-.0995
.60	.0204	.0296	.0323	.0350	.0341	.60	-.0571	-.0383	-.0434	-.0596	-.0795
.61	.0123	.0208	.0229	.0246	.0254	.61	-.0443	-.0248	-.0300	-.0439	-.0595
.62	.0042	.0120	.0140	.0158	.0172	.62	-.0315	-.0129	-.0182	-.0295	-.0394
.63	.0045	.0061	.0113	.0085	.0089	.63	-.0186	-.0039	-.0091	-.0156	-.0194
.64	.0108	.0208	.0280	.0226	.0090	.64	-.0121	-.0055	-.0052	-.0068	-.0119
.65	.0186	.0354	.0447	.0419	.0306	.65	-.0203	-.0143	-.0146	-.0172	-.0234
.66	.0278	.0501	.0614	.0612	.0523	.66	-.0284	-.0230	-.0240	-.0277	-.0349
.67	.0377	.0648	.0781	.0804	.0739	.67	-.0365	-.0318	-.0334	-.0381	-.0464
.68	.0483	.0794	.0949	.0997	.0956	.68	-.0447	-.0406	-.0428	-.0486	-.0579
.69	.0596	.0941	.1116	.1190	.1172	.69	-.0528	-.0493	-.0522	-.0590	-.0694
.70	.0716	.1088	.1283	.1382	.1389	.70	-.0610	-.0581	-.0616	-.0694	-.0809
.71	.0841	.1234	.1450	.1575	.1605	.71	-.0691	-.0668	-.0710	-.0799	-.0925
.72	.0969	.1381	.1617	.1768	.1821	.72	-.0772	-.0756	-.0803	-.0903	-.1040
.73	.1097	.1528	.1785	.1960	.2038	.73	-.0854	-.0844	-.0897	-.1008	-.1155
.74	.1226	.1674	.1952	.2153	.2254	.74	-.0935	-.0931	-.0991	-.1112	-.1270
.75	.1354	.1821	.2119	.2346	.2471	.75	-.1017	-.1019	-.1085	-.1217	-.1385
.76	.1482	.1968	.2286	.2538	.2687	.76	-.1098	-.1107	-.1179	-.1321	-.1500
.77	.1611	.2114	.2453	.2731	.2904	.77	-.1180	-.1194	-.1273	-.1426	-.1615
.78	.1739	.2261	.2621	.2924	.3120	.78	-.1261	-.1282	-.1367	-.1530	-.1730
.79	.1867	.2408	.2788	.3117	.3337	.79	-.1342	-.1370	-.1461	-.1635	-.1845
.80	.1996	.2554	.2955	.3309	.3553	.80	-.1424	-.1457	-.1554	-.1739	-.1960

END OF CALCULATIONS FOR THIS CASE

Figure 5.- Sample tabulation of the maximum and minimum hinge moments as a function of Mach number and hinge line location.

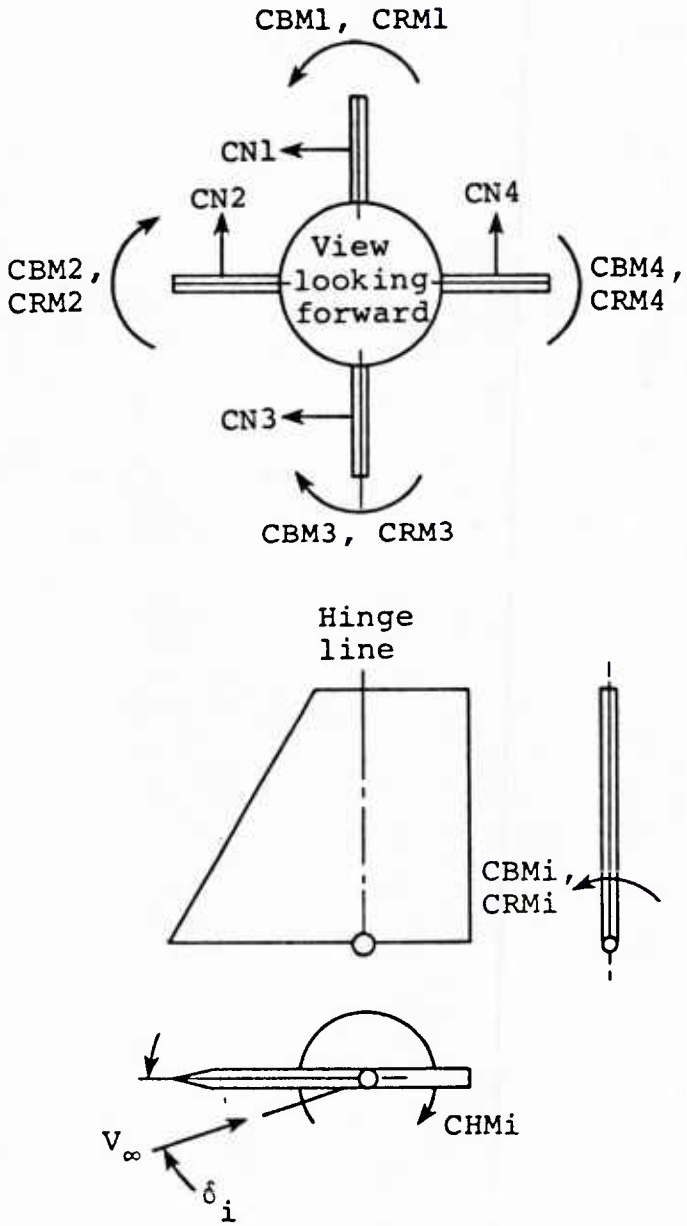

Figure 6.- Positive directions for canard fin force and moment coefficients.

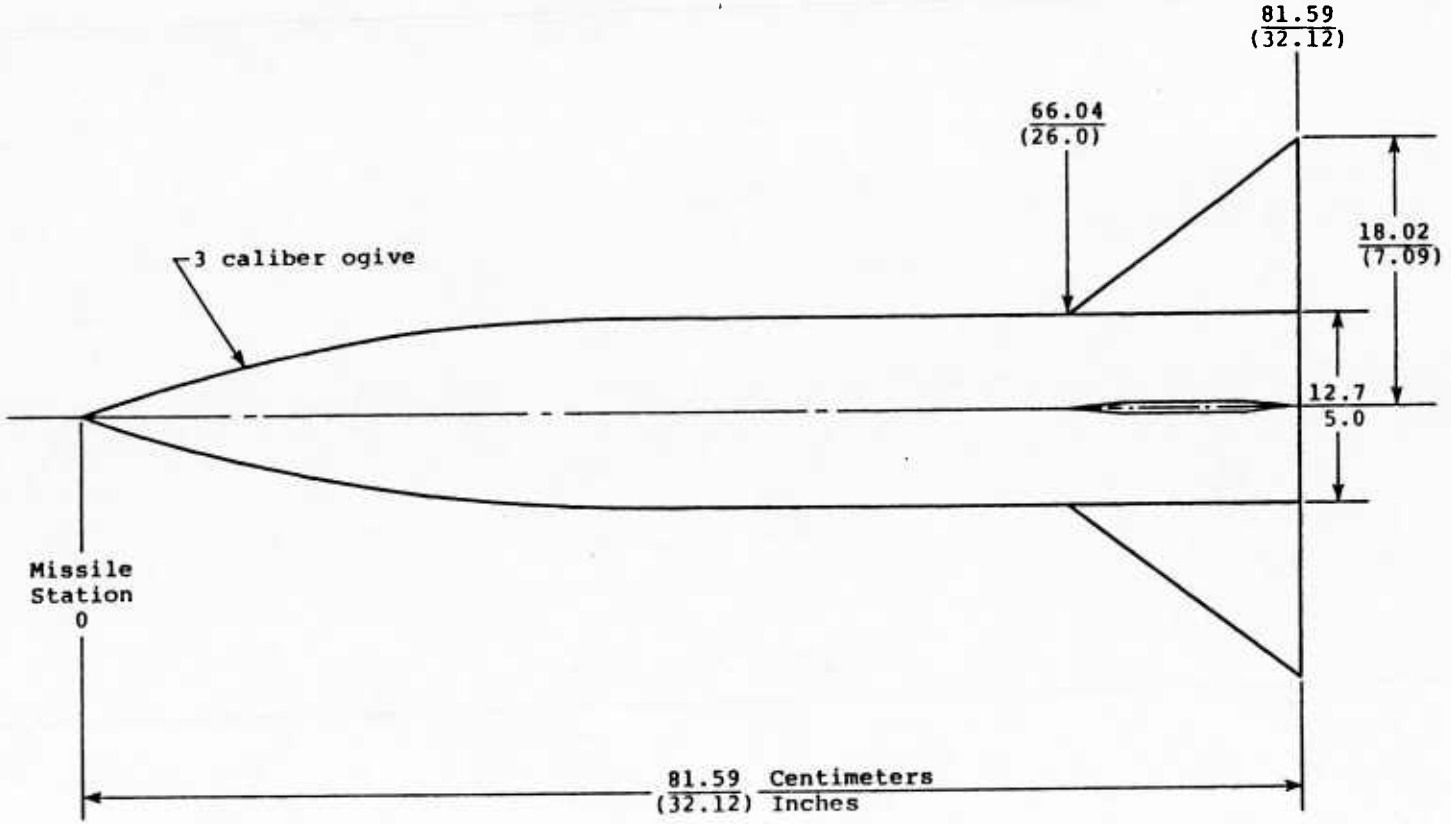

Figure 7.- Body-canard combination.

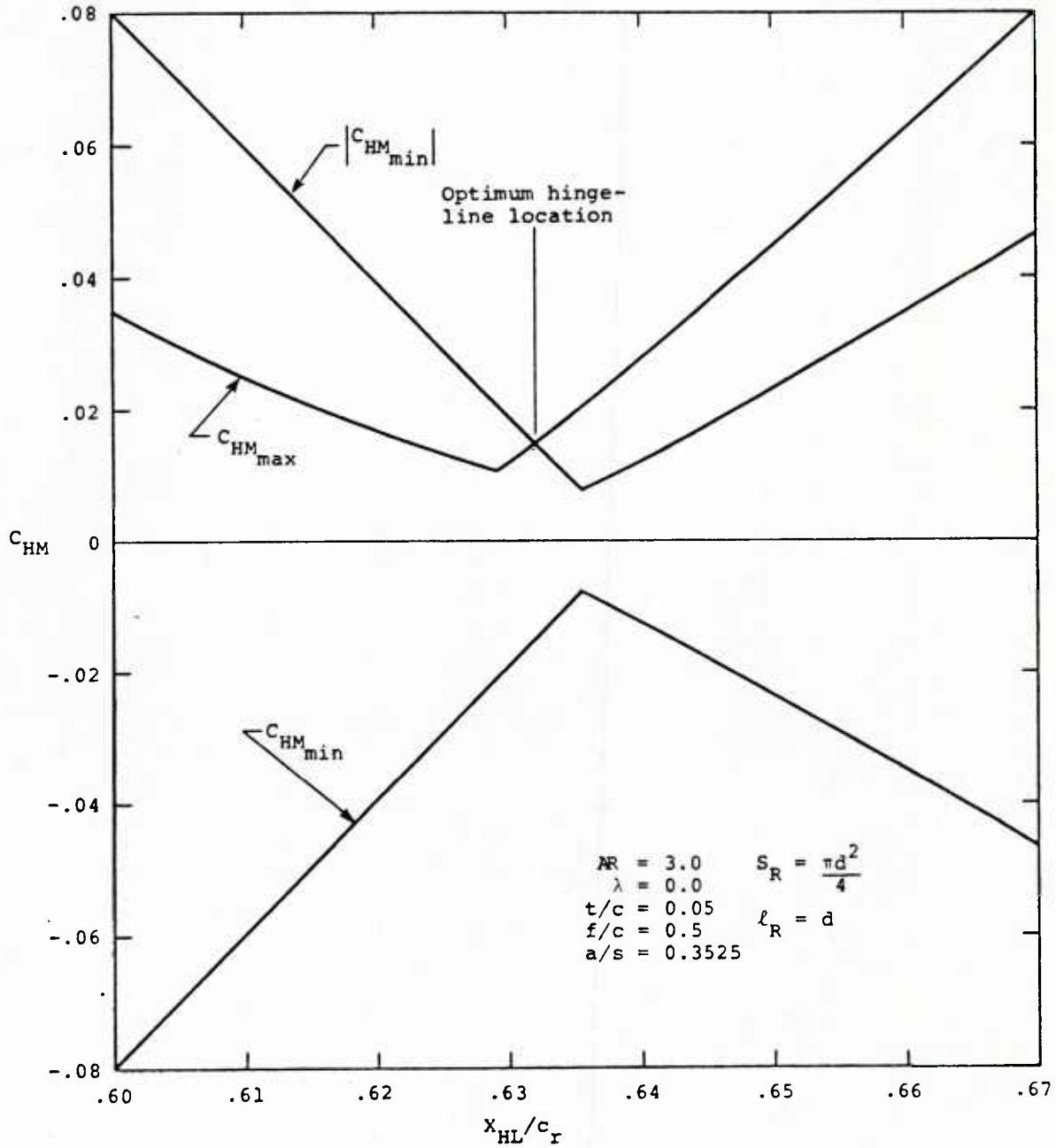

Figure 8.- Determination of optimum hinge-line location.

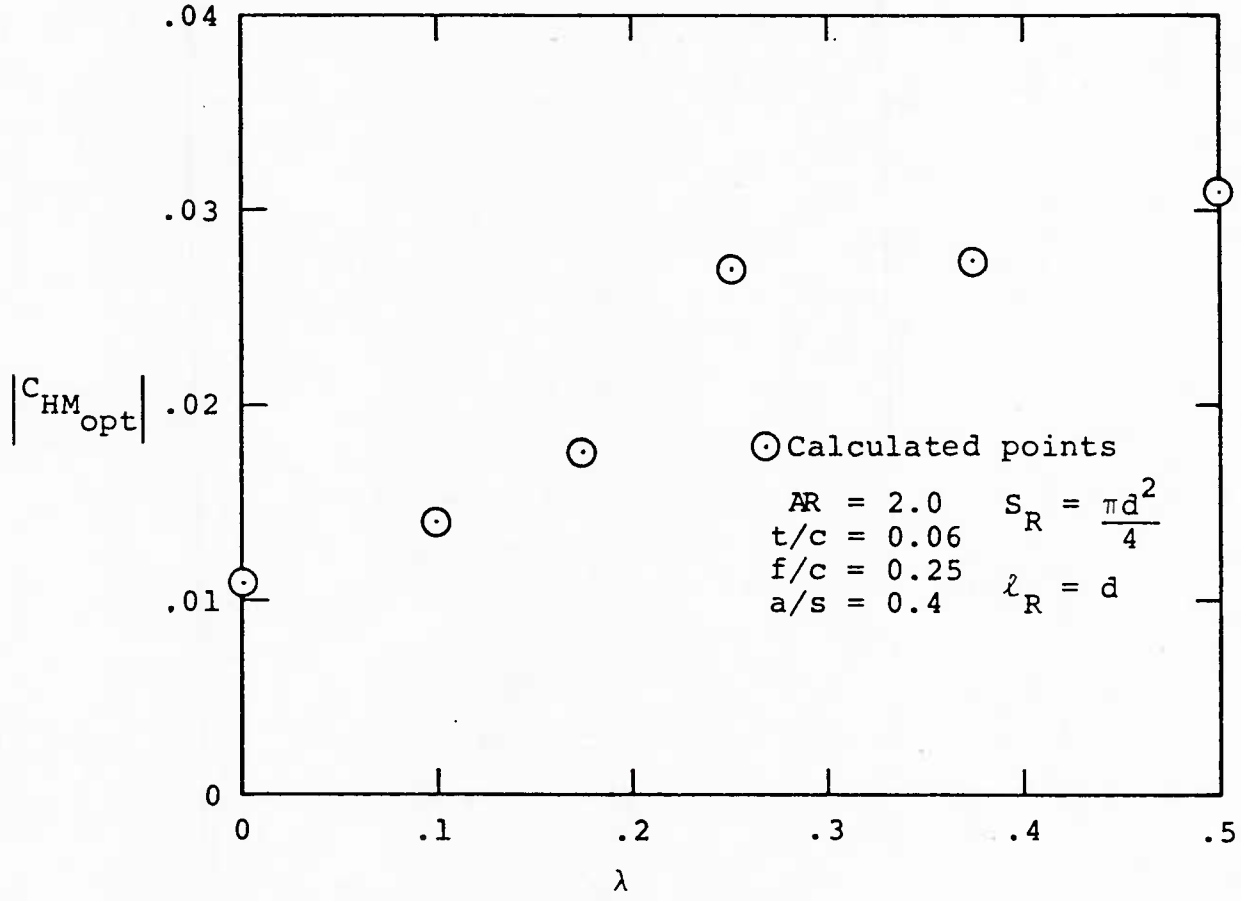

(a) AR = 2.0

Figure 9.- Variation with taper ratio of the magnitude of the maximum hinge-moment coefficient with the hinge line in the optimum location.

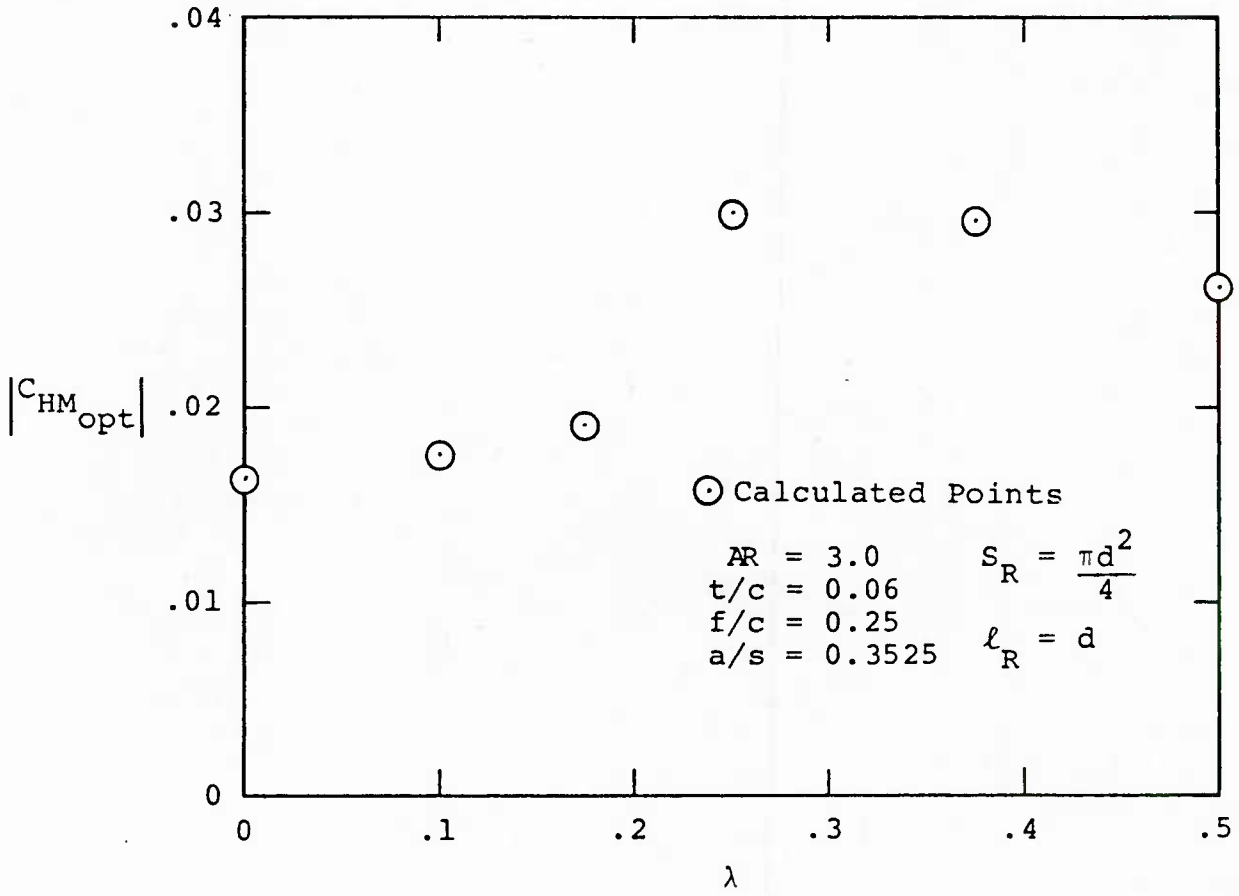

(b) AR = 3.0

Figure 9.- Concluded.

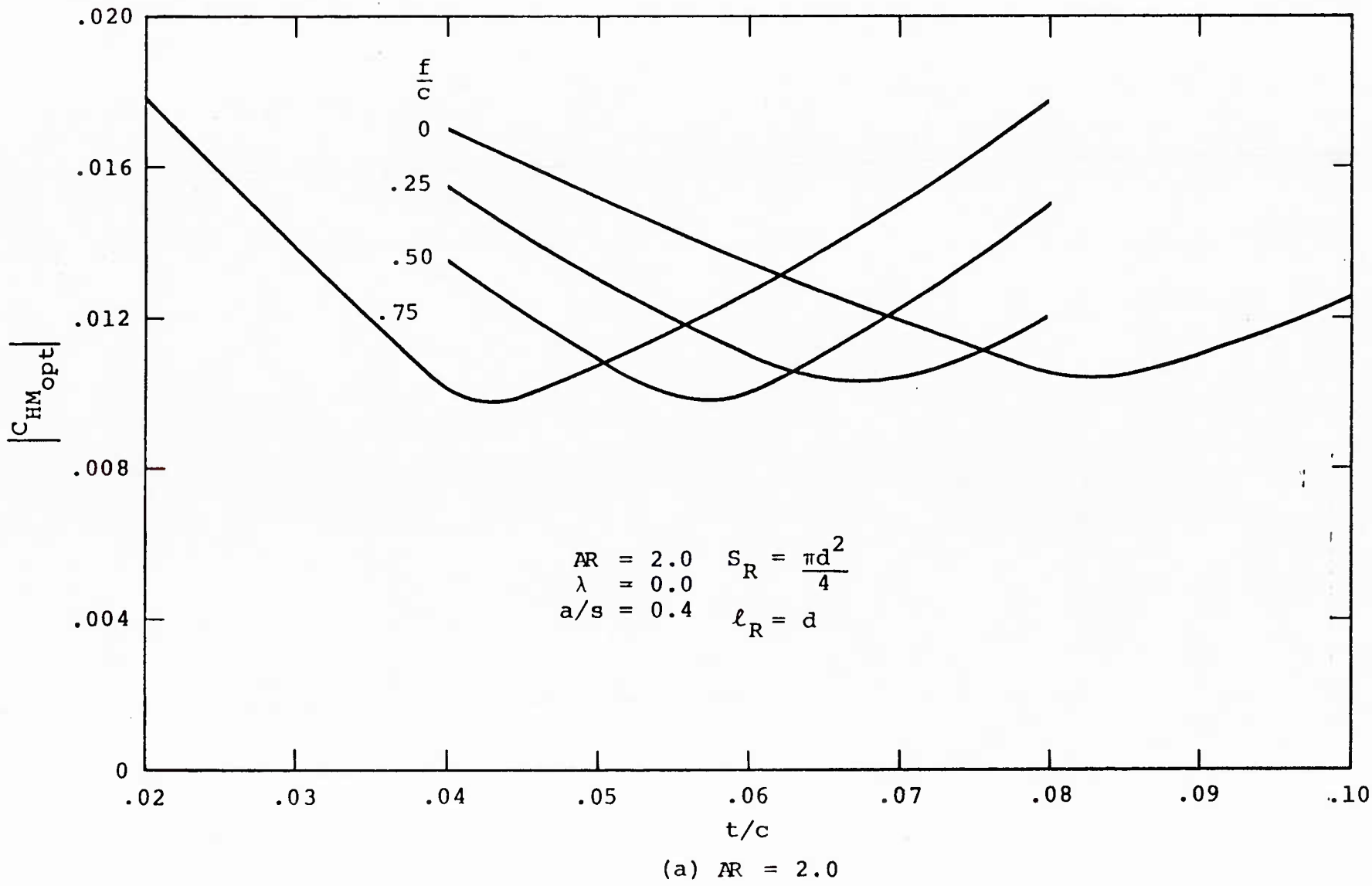

(a) AR = 2.0

Figure 10.- Variation with airfoil section parameters of the magnitude of the maximum hinge-moment coefficient with the hinge line in the optimum location.

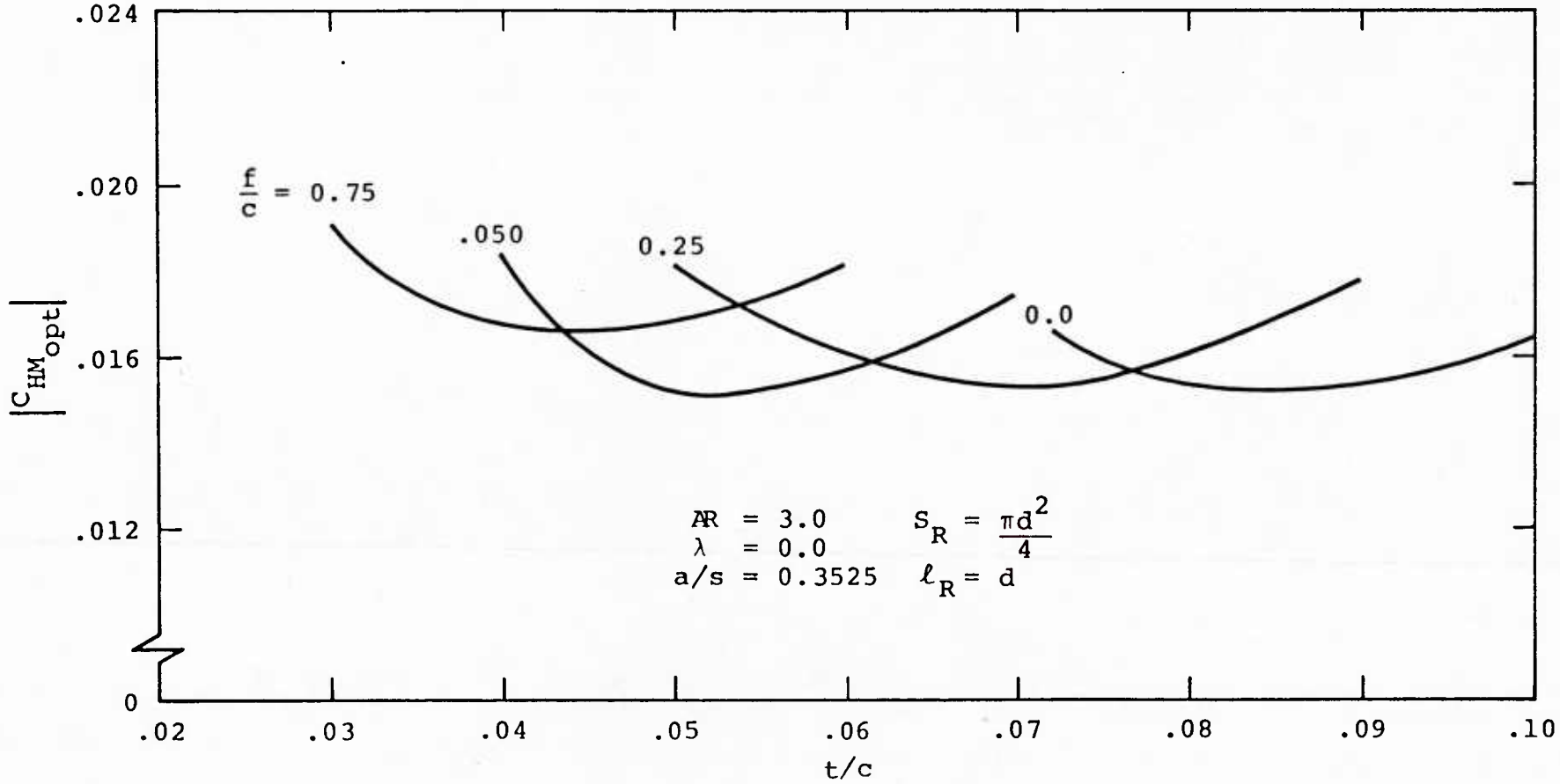

(b) AR = 3.0

Figure 10.- Concluded.

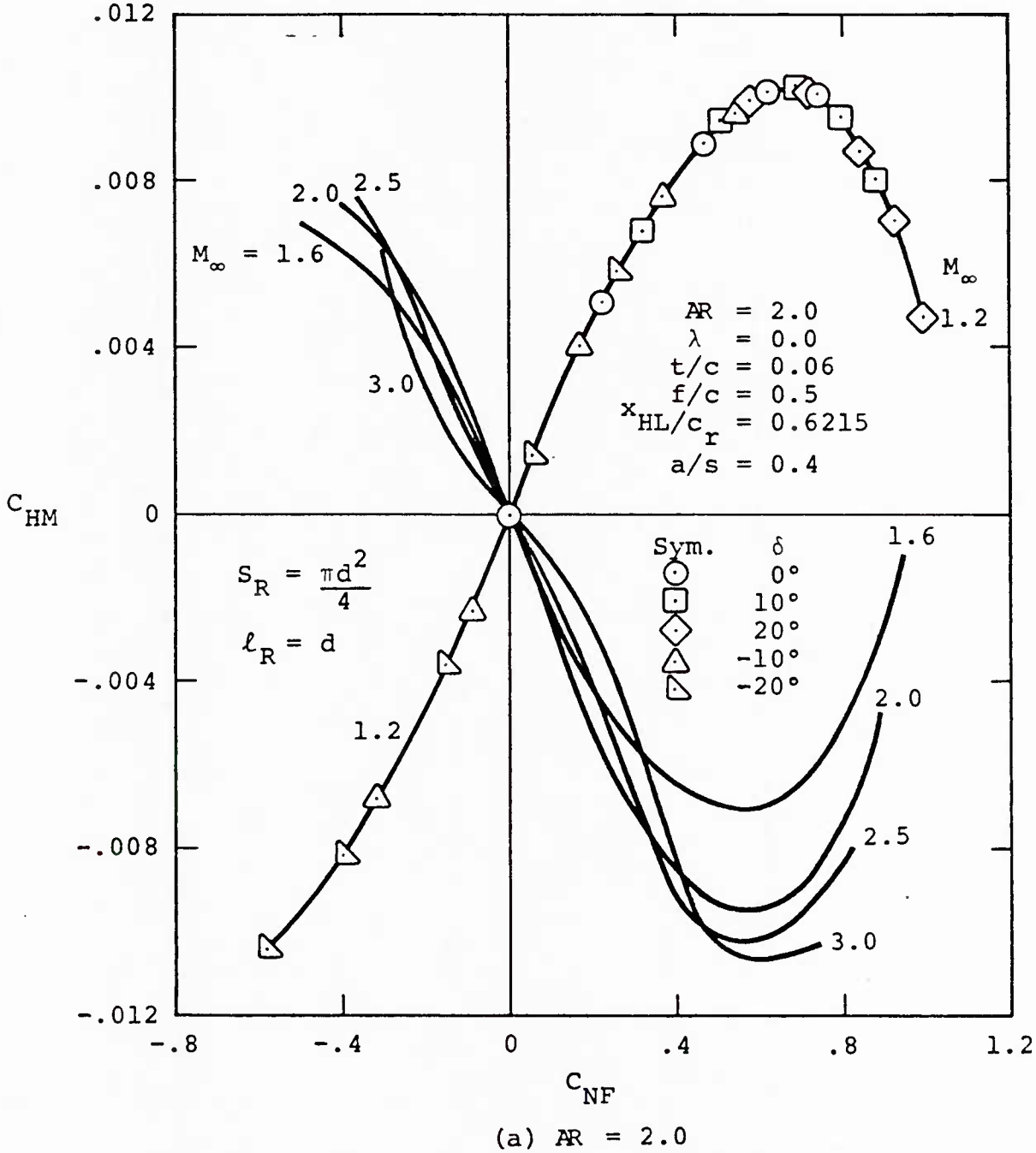

(a) AR = 2.0

Figure 11.- Variation of hinge-moment coefficient with fin normal-force coefficient for the optimum fins, $\phi = 0°$.

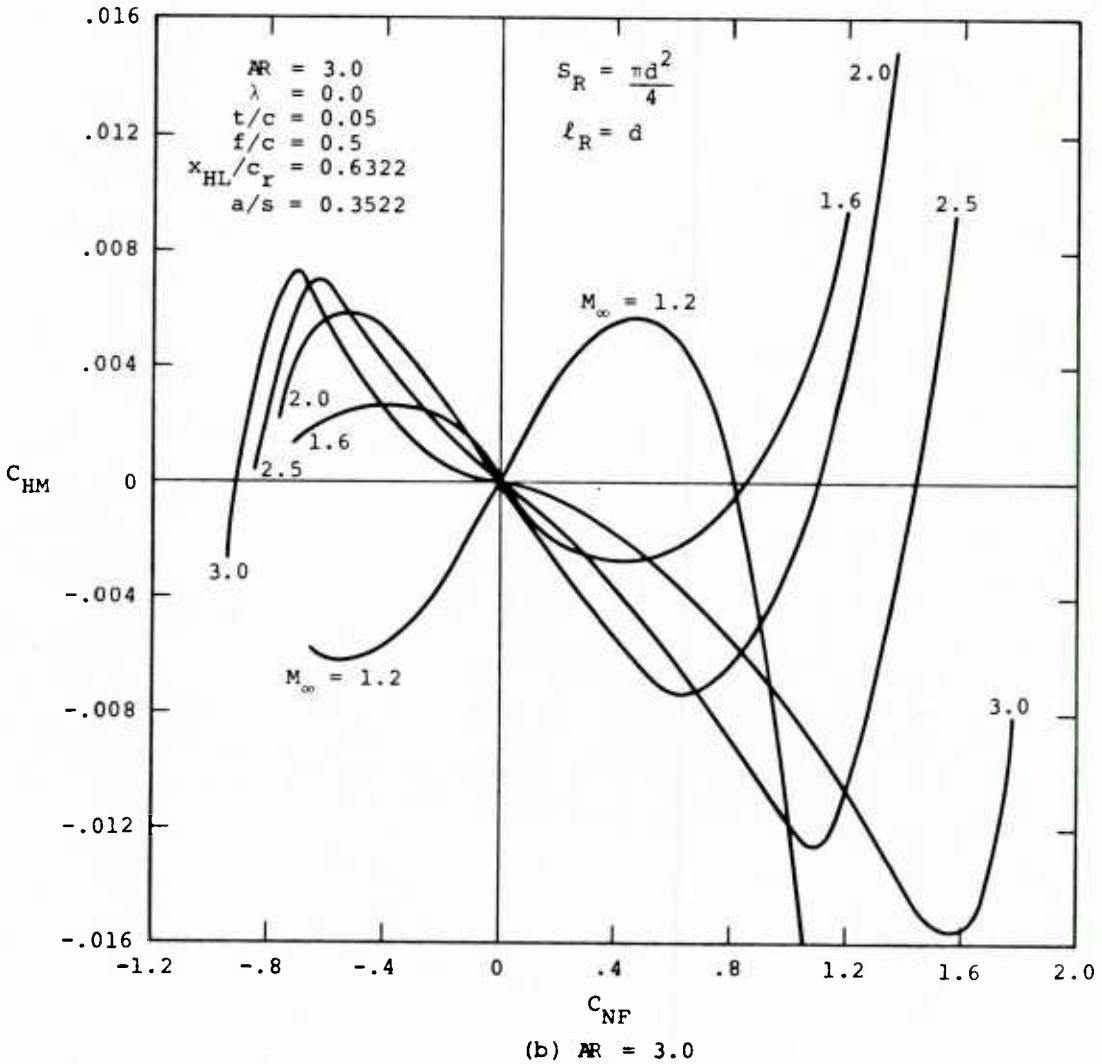

(b) AR = 3.0

Figure 11.- Concluded.

APPENDIX A

USER'S MANUAL FOR COMPUTER PROGRAM

A.1 INTRODUCTION

The purpose of this appendix is to describe the operation of the computer code in sufficient detail to permit understanding and use of the program. The program computes forces and moments for each section of the configuration, and for the complete configuration. Minimum drag is not computed. The code is capable of handling a body-canard or body-tail with no afterbody. A description of the engineering method is given in References A1, A2, and A3 and in the main text of this report.

The program is written in FORTRAN IV and has been run on the CDC 7600 and Cyber 760 machines. A typical running time for five Mach numbers, five canard deflection angles, five angles of attack, and one roll angle (125 points) is about 13 seconds on the CDC 7600 and about 19 seconds on the Cyber 760.

A.2 PROGRAM DESCRIPTION

For computational purposes, the missile to be studied is divided into two sections. The nose section is defined to be from the nose tip to the leading edge of the root chord of the finned section. The canard section (finned section) is defined to be from the end of the nose section to the trailing edge of the set of fins. The main program controls the flow of operations. It calls the routines which control the operations for each section of the missile. Figure A.1 shows the routines called by the main program and the routines which they in turn call.

A.2.1 Calculation Procedure

Figure A.2 shows the flow of the program computation. This figure and figure A.1, which shows the subprogram call sequence, are the basis for the following description of the calculation procedure.

Subroutine INPT reads in the run identification information, and then reads in body and fin geometry, run control parameters, and flow conditions. All length quantities are then normalized by the body radius and all areas are normalized by the square of the body radius.

After all the input has been read in, the required interference factors are computed by calling routines INTFAC, INFLU, and CCL. Next, routine WNGCNW is called to obtain the wing-alone normal-force coefficient, C_N, as a function of angle of attack, α, from the data base, for the input canard planform. Subroutines SHKEXP and XCPVSA are called to calculate the wing-alone longitudinal center of pressure, $\bar{x}/c_r$, as a function of α. This calculation includes the correction for thickness effects.

The next step in the calculation is to calculate the loads on the nose section. This is accomplished through calls to LNTRP and NOSE. LNTRP is used to determine some crossflow-drag quantities. NOSE first computes the axial starting location of the nose vortices (if present). The locations and strengths of the nose vortices in the crossflow plane at the leading edge of the root chord of the canard section are computed next. The subroutine then computes the forces and moments on the nose and returns control to the main program. The vortex positions and the forces and moments are printed in NOSE if the parameter NOUTPT = 1.

Subroutine CANARD is now called to calculate the canard loads and the body loads in the canard section. The individual fin forces and moments in the absence of the nose vortices are computed first. The user may choose to ignore the nose vortices

over the canards if he believes they have dispersed. This control is achieved throught the parameter NVORT.

If nose vortices are present over the finned section, subroutine REVFLO is then called by CANARD. Subroutine REVFLO computes the equivalent angle of attack and spanwise location of the center of pressure for the loading due to the nose vortices. Subroutine REVFLO assumes the vortices to be infinite line vortices parallel to the body axis.

When REVFLO returns control to CANARD, the total fin forces and moments and body forces and moments (for the canard section) are computed. The canard individual fin loads are always printed in CANARD. If the parameter NOUTPT = 1, additional output is printed. This includes the effect of hinge-line location on the fin hinge moments and the contribution of the canard section to the total loads.

Upon returning to the main program, a summary of the overall forces and moments is printed if NOUTPT = 1. Following this, a search through all canard deflection angle, δ, and angle of attack, α_c, combinations for this Mach number, M_∞, and roll angle, ϕ, is made to find, as a function of hinge-line location, the maximum and minimum hinge moments acting on fin 4. This fin is the right-horizontal fin, looking upstream at $\phi = 0°$. When $\phi = 0°$ the fins are vertical and horizontal.

After exiting from the Mach number loop, the maximum and minimum hinge moments acting on fin 4 are tabulated as a function of hinge-line location and Mach number. A separate table is printed for each roll angle.

A.2.2 Program Limitations and Precautions

The program makes a number of assumptions about the missile configuration and the flow field. These are described briefly below.

1. The fins in the canard section must be identical, uncambered and untwisted. Thickness effects are included and the fin airfoil sections must be similar across the span of the fin.

2. The leading edges of the fins must not be swept forward and the trailing edges must be unswept. If a fin with rectangular planform is to be modeled the user must set the leading-edge sweep to some small positive value. The procedure for doing this is described in section A.3.

3. The included angle of attack, α_c, should not exceed 45°.

4. The fin equivalent angle of attack should not exceed 60°.

5. The Mach number range of the data base in the program for fin normal-force coefficient is 0.8 to 3.0. The program cannot be run below a Mach number of 0.8 and probably should not be run below $M_\infty = 1.2$ because of strong transonic effects not accounted for in the methods. In the work of reference A3, the Mach number extrapolation scheme was changed so the extrapolation was done as $1/\sqrt{M_\infty^2 - 1}$. If was found there that, using data in the $M_\infty = 2$ to 3 range, the normal-force coefficient at $M_\infty = 4.6$ could be well predicted. Thus, the present program can probably be used up to $M_\infty = 4.5$ with some confidence.

6. The aspect ratio range of the data base in 0.5 to 3.53 for $0.8 \leq M_\infty \leq 1.3$ and 0.5 to 2.0 for $1.3 \leq M_\infty \leq 3.0$. The program will extrapolate beyond the data base to include fins with aspect ratio less than 0.5 but it is recommended that such fins not be used. This is because of the large variation in loads with aspect ratio in this range. In the work of Reference A3 the aspect ratio extrapolation to aspect ratios, AR, greater than 2.0 was changed from linearly extrapolating in AR to extrapolating as 1/AR. It was found there that the normal-force coefficient for an AR = 4.0 fin could be predicted quite well using AR = 1.0 and 2.0 data. Therefore, the present program can probably be used for aspect ratios up to 4.0.

A.2.3 Description of Subroutines

The main program primarily acts as an executive routine. It calls the other subroutines as needed and totals the loads from each section.

Subroutine BUSEMN uses Busemann's second-order theory to calculate the center-of-pressure shift due to the fin airfoil thickness distribution. It is described on page 243 of Reference A4.

Subroutine BVTEX computes nose vortex positions and strengths.

Subroutine CANARD controls the subroutines which compute vortex strengths and positions, individual fin forces and moments, body forces and moments, and total forces and moments for the canard section.

Subroutine CCL computes the fin influence coefficients used in the reverse flow procedure.

Function CHRT8 calculates the fin lift-curve slope at supersonic speeds from the curves of Chart 8 of Reference A5. This subroutine, as well as some of the other subroutines are documented in Reference A6.

Subroutine CH1416 calculates the center of pressure of the lift carryover onto the body due to the canard from the curves of Charts 14, 15, and 16 of Reference A5. This subroutine is documented in Reference A6.

Subroutine CLAM calculates the fin-fin interference factors used in determining the change in equivalent angle of attack due to fin deflection.

Functions CNT6, CNT11, CNT14, CNT15, CNT23, and CNT31 compute the vortex-free normal-force coefficient for fins in the data base. These data are contained in tables 8 and 9 of Reference A1.

Subroutine CURVES is a block data routine for initializing a number of empirical tables used in the program.

Function EQ30 calculates the value of $K_{B(C)}(\beta C_{N_\alpha})_C$ using equation (30) of Reference A5. This function is used for the high-aspect-ratio range at supersonic speeds when there is no afterbody behind the finned section and βm is greater than one. This subroutine is documented in Reference A6.

Function EQ31 is similar to EQ30 and is used when βm is less than one.

Subroutines FINTML, FINTMR, FINTNL, and FINTNR compute integrands used in the reverse-flow procedure by CCL. These integrands are discussed in Appendices A and B of Reference A1.

Subroutines IBCIEU, ICSEVU, and ICSICU are routines used for cubic spline interpolation in the data base.

Subroutine INFLU computes the effects of Mach number on panel-panel interference.

Subroutine INPT reads and prints all input data and non-dimensionalizes it.

Subroutine INT performs linear interpolation in a three dimensional array of data.

Subroutine INTFAC calculates interference factors by the method of slender body theory or the methods of Reference A5.

Subroutine LNTRP is a linear interpolation routine.

Subroutine NOSE computes forces and moments on the nose section and the positions and strengths of the nose vortices, if any, at the canard root-chord leading edge.

Subroutine REVFLO computes the equivalent angles of attack and spanwise locations of the centers of pressure for a set of fins due to the presence of vortices.

Subroutine SHKAGL calculates the shock-wave angle associated with a wedge of a given angle using the method of Appendix B of Reference A3.

Subroutine SHKEXP calculates the center-of-pressure shift due to fin thickness using shock-expansion theory by the method of Appendix B of Reference A3.

Subroutine SIMP1 is a Simpson's Rule integration package used by CCL.

Subroutine SIMSON is a Simpson's Rule integration package used by REVFLO.

Subroutine VEL calculates the velocity at several points spanwise along a fin induced by external vortices.

Function WNGCNT computes the vortex-free, normal-force coefficient for a general fin from the data base contained in functions CNT6, CNT11, CNT14, CNT15, CNT23, and CNT31.

Subroutine WNGCNW computes the wing-alone normal-force coefficient for a fin. The data used are contained in tables 2 and 3 of Reference A1.

Function XBAR computes the chordwise location of the fin center of pressure from the table calculated in subroutine XCPVSA.

Subroutine XCPVSA calculates a table of chordwise locations of the fin center of pressure as a function of angle of attack including thickness effects.

Function YTAB computes the spanwise location of the fin center of pressure from the data base given in tables 4 and 5 of Reference A1.

A chart listing which common blocks are in each subroutine is given in figure A.3.

A.3 DESCRIPTION OF INPUT

This section describes the input required by the computer program. Included is a discussion of any constraints on the value or use of the variables and, where appropriate, suggested values. Basically, there are three types of variables; geometric, flow,

and program control. In addition, the order in which the input variables are read approximately corresponds to the geometric order of the various sections of a missile. That is, the information required by the nose section is entered first, followed by the information for the canard section.

The program has been designed to study several different configurations consecutively. Thus, the input decks for each of the configurations can be stacked together, with the exception of item 12, and the program will analyze each configuration in order. Item 12 is the last card of the input deck and indicates the end of information. All input variables are listed and defined in the next section in the order of appearance in the input deck. The input formats are shown in figure A.4. The item numbers below also refer to that figure. A sample input case is discussed in section A.6.

Item 1

These cards provide identification of the run. The first card contains the index NCARDS which indicates how many cards of information follow to describe the run. The value of NCARDS must be one or greater.

Item 2

This item provides run control information. The first variable, NMACH, specifies the number of values of the Mach number, M_∞, for which calculations are to be made. The value of NMACH must be between one and five.

The second variable, NDELT, specifies the number of sets of canard fin deflection angles, δ_i, i = 1,2,3,4, for which calculations are to be made. The value of NDELT must be between one and five.

The third variable, NALFA, specifies the number of values of the angle of attack, α_c, at which calculations are to be made. The value of NALFA must be between one and ten.

The fourth variable, NPHI, indicates the number of roll angles, ϕ, for which calculations are to be made. The value of NPHI must be between one and ten.

The computer program consists of a quadruple do loop as shown in figure A.2. Thus, the total number of conditions for which calculations are made is the product of these four variables.

The fifth variable, NI, is the number of integration intervals plus one, used in the Simpson's rule integration routine called by REVFLO. The value of NI must be odd. A suitable value for NI depends on how close a vortex is to a fin. If a vortex is close to a fin, the value of NI should be at lease 51. Since REVFLO uses only a small fraction of the total run time, it is recommended that NI be set equal to 99, the maximum possible value.

The sixth variable, NNOSE, is equal to the number of entries in the table of nose coordinates. The first value is the distance of the nose tip from missile station zero and the last value is the location of the shoulder. The value of NNOSE must be between two and twenty.

The seventh variable, NCA, indicates whether the slope of the linear normal-force curve, C_{N_α}, for the nose is to be read in. If NCA equals zero, then C_{N_α} is assigned the value 2.0 by the program. This is the value predicted by slender-body theory. If NCA $\neq$ 0, a value for C_{N_α} is to be read in later.

The eighth variable, NVORT, is used to control the influence of the nose vortices. It has been observed (Refs. A7 and A8) that nose vorticity for $\alpha_c \leq 20°$ may disperse over the canard section. Since the present model for nose vorticity is incapable of representing such a situation, the user has the option of

ignoring the influence of nose vorticity downstream of the canard root-chord leading edge. The options are:

NVORT = 1: nose vortices are ignored downstream of the leading edge of the canard root chord

NVORT = 2: nose vortices are included to the trailing edge of the canard

The ninth variable, NOUTPT, controls the amount of output produced by the program. If NOUTPT = 0, the canard fin forces and moments are tabulated as well as the final summary tables of the maximum and minimum hinge moments. If NOUTPT = 1, the above is printed as well as the nose vortex strengths and positions, the nose section forces and moments, additional canard fin information, the total canard section forces and moments, and the total configuration forces and moments.

The tenth variable, logical variable TURB, is used to determine which branch of the crossflow drag coefficient table is to be used. For crossflow Mach numbers below 0.6, the laminar and turbulent values of c_{d_c} differ. If there is doubt about which type of flow separation is present, use TURB=.TRUE., turbulent flow.

The eleventh variable, logical variable REFER, is used to control the reference areas and lengths for the fin output. If REFER = .TRUE., the reference area for the fin loads is the fin planform area, the reference length for fin hinge moments is the fin root chord, and the reference length for fin root-bending moments and rolling moments is the exposed span of the fin. If REFER = .FALSE., the input reference area and length are used for the fin output as well as for the overall loads.

Item 3

This item provides some geometric information. The first two variables, LROUT and SROUT, are the reference length and reference area, respectively. The next variable is XMC, the

moment center measured from missile station zero (MSO). The variable A is the radius of the cylindrical section of the missile.

The variables TIPRAD and ETAN are entered next. The variable TIPRAD is the radius of the spherical nose tip. If the nose is pointed, then ETAN is the nose half-angle. If the nose is blunted, then ETAN is the angle between the body axis and the tangent to the nose at the juncture of the spherical cap and the rest of the nose.

The variable XCLE is the distance from missile station zero (MSO) to the leading edge of the root chord of the canard fins. Any dimensional system is acceptable. However, one must be careful to use the chosen system consistently.

Item 4

This item contains the NMACH values of the Mach number for which computations are to be performed.

Item 5

The variable DCNDA is the slope of the nose normal-force coefficient curve due to attached flow. The reference area is the base of the nose. This item is included only if the value of NCA in Item 2 was set equal to a value different than zero.

Item 6

This item contains the nose coordinates. First the axial positions, XNOSE, are entered, followed by the corresponding values of the local nose radius, RNOSE. There should be NNOSE values of each. The values of XNOSE are measured from missile station zero.

Item 7

This item contains the NALFA values of the angle of attack for which computations are to be performed.

Item 8

This item contains the NPHI values of the role angle for which computations are to be made.

Item 9

This item is a set of NDELT cards. Each card of this item contains the fin deflection angles for the four canard fins. As viewed from the rear, for $\phi = 0°$, δ_1, and δ_3 (vertical fins) are positive for trailing edges to the right and δ_2 and δ_4 (horizontal fins) are positive for trailing edges down. At $\phi = 0°$, fin 1 is on top and the fins are numbered counterclockwise.

Item 10

This item is one card and contains geometric information about the canard section. The first variable, SPANC, is the fin semispan measured from the body axis. The next three variables, XCHL, XCTIPL, and XCTE, are the axial positions of the hinge line, the leading edge of the tip chord, and the trailing edge, respectively. These three axial positions, as well as all other axial positions, are measured from MSO. Recall from section A.2.2 that the leading-edge sweep cannot be zero, even for a rectangular planform. For the case of a rectangular planform set XCTIPL greater than XCLE by a small number, for example 0.01.

Item 11

This item contains the data required to calculate the chordwise center-of-pressure shift due to fin thickness. The first variable, NFOILS, is the number of strips across the span which the fin is to be divided into. It must be between one and ten. For a rectangular fin, one can be used. For other fins, five or six is sufficient. The last two variables of this item, TOC and FOC, specify the airfoil section which is similar across the span of the fin. The program treats an airfoil which is a flat plate with equal length leading and trailing edge wedges. the variable TOC is the ratio of the flat-plate thickness to the airfoil chord while FOC is the ratio of the length of the flat section to the

airfoil chord. FOC can be zero, a double wedge airfoil, and cannot be one.

This is the last card of input for a case. If an additional case(s) is to be included in this run, start over with Item 1. Otherwise add Item 12.

Item 12

This card ends the process of entering data. It has 999 punched in columns 3, 4, and 5. It should be the last card and follow all the data cards for the case(s) to be run. The computer program stops the search for more data and the run is completed.

A.4 SYMBOL LISTING

Program Variable	
Item 1	Alphanumeric information to identify the run.
NCARDS	Number of cards used to identify the run; NCARDS $\geq$ 1.
HEAD(I)	NCARDS cards of alphanumeric information for identification of the run; 1 $\leq$ I $\leq$ NCARDS.
Item 2	Integer and logical variables for control of program operation.
NMACH	Number of Mach numbers for which calculations are to be made; 1 $\leq$ NMACH $\leq$ 5.
NDELT	Number of sets of canard fin deflection angles for which calculations are to be made; 1 $\leq$ NDELT $\leq$ 5.
NALFA	Number of angles of attack for which calculations are to be made; 1 $\leq$ NALFA $\leq$ 10.
NPHI	Number of roll angles for which calculations are to be made; 1 $\leq$ NPHI $\leq$ 10.
NI	One plus the number of intervals to be used in the Simpson's rule integration package in REVFLO; must be odd; 1 $\leq$ NI $\leq$ 99.

Program Variable	
NNOSE	Number of entries in the table of nose coordinates; $2 \leq$ NNOSE ≤ 20.
NCA	Integer flag specifying whether C_{N_α} of nose is to be entered. NCA = 0: C_{N_α} not entered. NCA $\neq$ 0: C_{N_α} entered.
NVORT	Integer flag indicating how far along body influence of nose vortices is to be felt. NVORT = 1: influence of nose vortices felt up to leading edge of canard root chord. NVORT = 2: influence of nose vortices felt up to trailing edge of canard root chord.
NOUTPT	Integer flag controlling amount of output. NOUTPT = 0: only fin loads and maximum and minimum hinge moments are output. NOUTPT = 1: complete output.
TURB	Logical variable stating whether crossflow on body is laminar or turbulent. TURB = .TRUE.: crossflow is turbulent. TURB = .FALSE.: crossflow is laminar.
REFER	Logical variable concerning output reference areas and lengths for fins. REFER = .TRUE.: use fin planform area, root chord and exposed semispan. REFER = .FALSE.: use input reference area and reference length.
Item 3	Reference and geometric information.
LROUT (ℓ_{ref})	Reference length used in moment calculations.
SROUT (S_{ref})	Reference area used in force and moment calculations.
XMC (x_m)	Moment center of missile measured from missile station zero, dimensional.
A (a)	Radius of missile, dimensional.
TIPRAD	Nose tip radius, dimensional.

ETAN (η) — Half angle of body nose for pointed body; or angle between tangent to nose at juncture of spherical cap and rest of nose and body axis, degrees.

XCLE — Distance from missile station zero to leading edge of canard root chord, dimensional.

Item 4

CMACH(J), (M_∞(J)) — Free-stream Mach number; 1 $\leq$ J $\leq$ NMACH.

Item 5

XNOSE(M) — Axial location entries in nose coordinate table; 1 $\leq$ M $\leq$ NNOSE; XNOSE(1) is axial location of nose tip from MS 0, dimensional.

RNOSE(M) — Corresponding radial location entries in nose coordinate table; 1 $\leq$ M $\leq$ NNOSE, dimensional.

Item 7

ALFAC(K), (α_c(K)) — Body angle of attack in degrees; 1 $\leq$ K $\leq$ NALFA.

Item 8

PHI(L), (ϕ(L)) — Bank angle in degrees; angle between z and z_o axes; positive measured clockwise viewed from rear; 1 $\leq$ L $\leq$ NPHI.

Item 9

DEFC(I,J), (δ_c(I)) — *Jth* set of canard fin deflection angles, degrees. 1 $\leq$ I $\leq$ 4; number of the canard fin. 1 $\leq$ J $\leq$ NDELT.

Item 10 — Canard geometry.

SPANC(s_m) — Maximum semispan, measured from body centerline, of canard fins, dimensional.

XCHL (x_{HL}) — Axial distance to canard hinge line, meausred from MS 0, dimensional.

XCTIPL — Axial distance to leading edge of canard tip chord, measured from MS 0, dimensional; XCTIPL > XCLE.

XCTE — Axial distance to canard trailing edge, measured from MS 0, dimensional.

Item 11	Fin airfoil data
NFOILS	Number of strips across span which the fin is to be divided into; $1 \leq$ NFOILS ≤ 10.
TOC (t/c)	Ratio of flat-plate thickness to airfoil chord length.
FOC (f/c)	Ratio of flat-plate length to airfoil chord length.
Item 12	
999	This card causes the program to stop searching for more data and the run is stopped.

A.6 SAMPLE CASE INPUT DATA

The input data for a sample case is presented in this section to illustrate the use of the computer program. The configuration used is shown in figures A.5 and A.6. The body used is N1B from Reference A7 but is terminated at the canard trailing edge. The canard fin is one of the fins used in the parametric study for the present report.

The input data deck for this case is shown in figure A.7. The calculation is done for five Mach numbers, five sets of fin deflection angles, five angles of attack, and one roll angle. Eleven points are used in the Simpson's rule integrations in subroutine REVFLO and there are 16 entries in the nose shape table. The nose normal-force-curve slope is not input (NCA = 0) and the influence of nose vortices is calculated to the canard root-chord leading edge (NVORT = 1). The option of printing only the fin loads and the maximum and minimum hinge-moment tables is selected (NOUTPT = 0). The crossflow is considered turbulent (TURB = T) and the input reference area and reference length are used for the fin loads (REFER = F).

A.7 DESCRIPTION OF OUTPUT

This section of the report will describe the output from the program. The output for the sample case will be used for this

purpose. This is shown in figure A.8. Not all of the output is included in the figure. Sufficient is presented to describe everything and also to verify that the program is working properly.

The first section of output is the input data and is shown in figure A.8(a). The user provided heading information is first printed. This is followed by the missile geometry and the reference lengths and areas. The quantities CPXRC and CPYRC are the canard root chord and exposed span, respectively. The remaining output in the figure are the flight condition parameters and program operation indices. All of this is printed for both output options, NOUTPT = 0 or 1, at the beginning of each case.

The second section of output is shown in figure A.8(b). Here the fin-alone normal-force curve and center-of-pressure curve are tabulated for a particular Mach number. This information is printed each time the Mach number changes. The normal-force curve is obtained from the data base in the program. The center-of-pressure location as a fraction of the root chord (CR) is calculated in subroutine XCPVSA. For this case the leading-edge shock wave is detached so the Busemann theory is used for the thickness correction at $\alpha = 2°$. If the shock is attached, shock-expansion theory is used at the low angles of attack and is so indicated in the output. The $\alpha = 45°$ value is obtained from the data base in the program. This output is printed for both output options.

Figure A.8(c) shows the canard fin force and moment output for NOUTPT = 0. At the top of the page the Mach number, canard deflection angles, and roll angle are printed. This is followed by the canard fin forces and moments for each of the angles of attack, in this case five angles. For each angle of attack, the canard-fin nose-vortex-induced equivalent angle of attack (DALFEQ)V is tabulated as are the vortex induced normal-force coefficient (DCN)V, root-bending-moment coefficient (DCBM)V, hinge-moment coefficient (DCHM)V, and rolling-moment coefficient (DCRM)V. These are followed by the total canard-fin equivalent angle of attack ALFEQ and the normal-force CNF, root-bending-moment CBM,

hinge-moment CHM, and rolling-moment CRM coefficients. The last column lists the fin center-of-pressure location as a fraction of the root chord. All of the coefficients use SROUT and LROUT, input quantities, as the reference area and reference length. The positive directions of the force and moment coefficients are shown in figure A.9. A page of output like this is printed for each Mach number, fin-deflection angle, and roll angle combination for output option NOUTPT = 0, the one used in the sample case.

When the NOUTPT = 1 output option is used, the output for each angle of attack is expanded. An example for the $\alpha = 20°$ point shown in figure A.8(c) is presented in figure A.8(d). Output like this is printed for each Mach number, canard deflection angle, roll angle, and angle of attack combination. For the sample case this would be 125 pages of output like that shown in figure A.8(d).

At the top of the page the Mach number, canard deflection angles, and roll angle are listed. This is followed by the results for the nose section. The strengths and positions of the nose vortices at the canard root-chord leading edge are tabulated. The strengths are nondimensionalized by $2\pi V_\infty a$ and the positions in the x_o, y_o, z_o coordinate system by the body radius, a. The coordinate system is shown in figure A.10. The last nose section data tabulated are the forces and moments in the unrolled (x_o, y_o, z_o) coordinate system. Positive directions of the forces and moments are shown in figure A.10.

The first output printed for the canard section is that which was tabulated for the NOUTPT = 0 option, the fin loads made dimensionless by SROUT and LROUT. This is followed by a listing of fin hinge-moment coefficient as a function of hinge-line location. The hinge-line location is listed as a fraction of the fin root-chord length. The next output again lists the fin forces and moments but this time the nondimensionalizing quantities are the fin planform area, root chord, and exposed semispan. The final output tabulated for the canard section are the canard section contributions to the total loads. These include body loads.

The forces and moments are tabulated in the unrolled coordinate system (x_o, y_o, z_o) and rolled, or body-axis, system (x, y, z) shown in figure A.10.

The final output tabulated in figure A.8(d) is a summary of the total loads on the configuration. The nose loads, canard section loads, and the sum of these two are listed.

The last output printed for both output options is shown in figure A.8(e). This is a tabulation of the maximum and minimum hinge-moment coefficients for fin 4 as a function of hinge-line position and Mach number. A table like this is printed for each roll angle. The values listed are obtained, for each hinge-line location and Mach number, by searching through all of the angle of attack and fin-deflection angle combinations for which calculations were made.

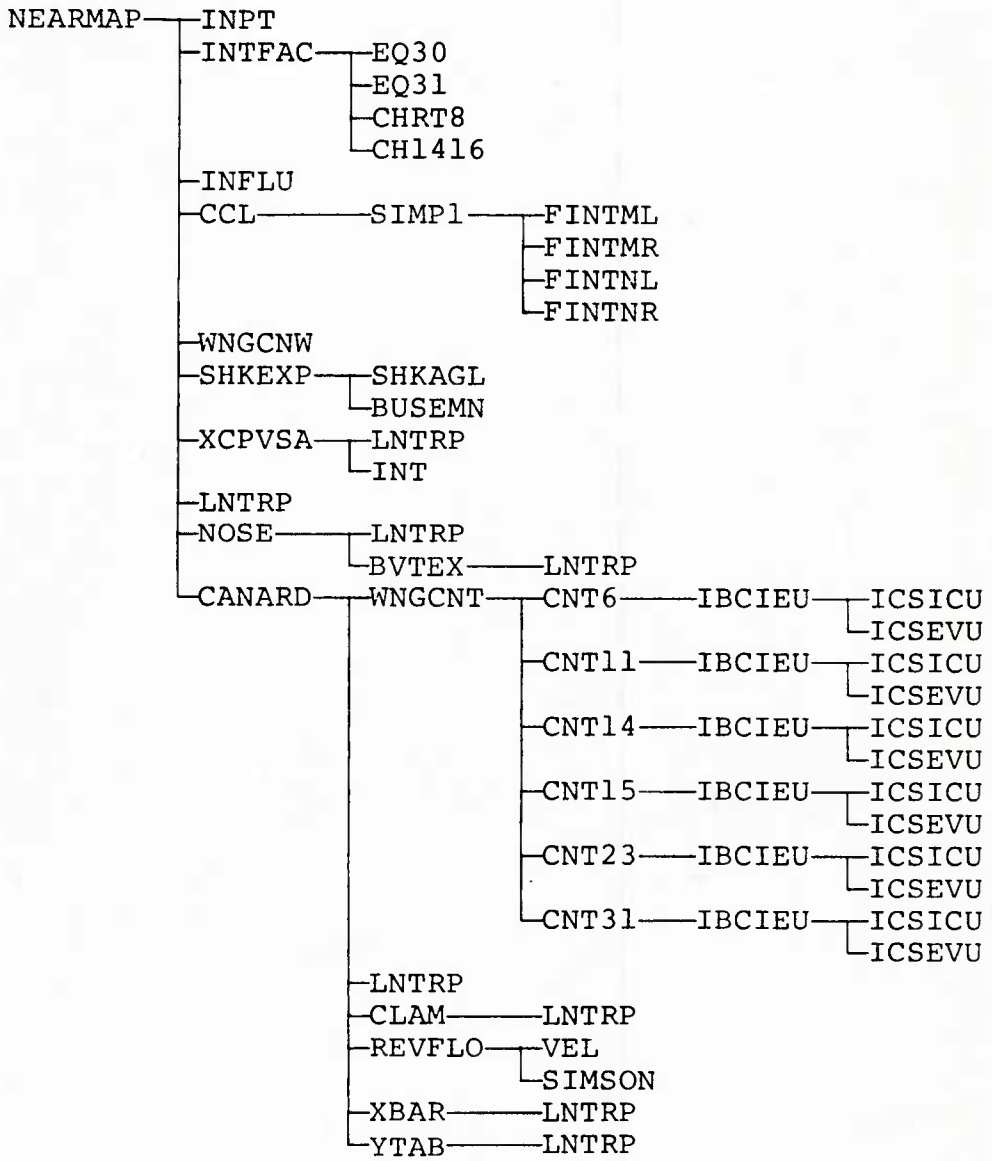

Figure A.1.- Routines called by main program and routines which they, in turn, call.

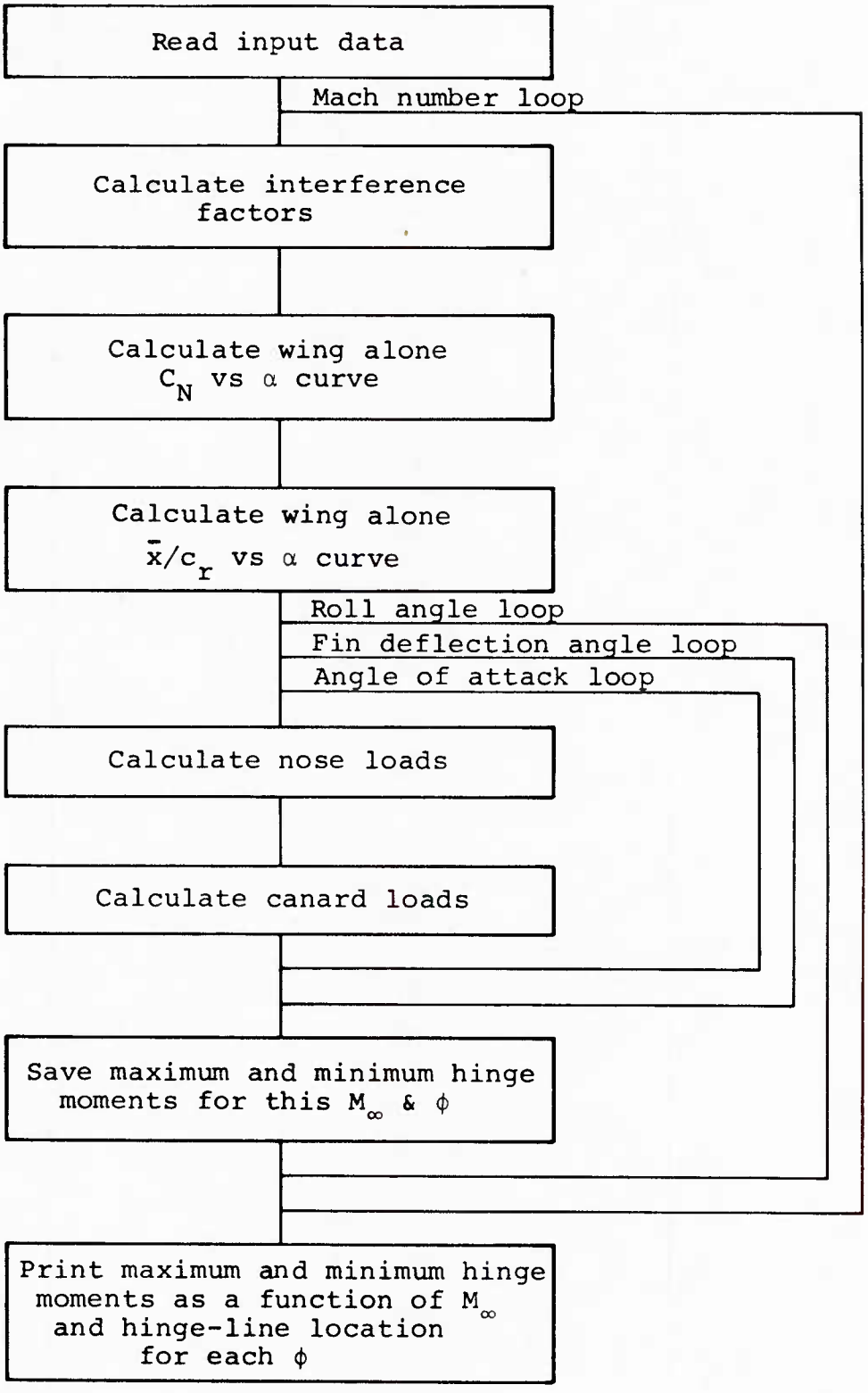

Figure A.2.- Flow of program computations.

ROUTINES	COMMON BLOCKS																	
	CAFT	CBODY	CCL	CFLT	CKFACS	CLDS	COP	CPCOM	CVRTX	DEFLC	FOILTK	INCOEF	LEEDRG	MACHDT	NOSDTA	SAVDAT	WING
NEARMP	X	X		X	X	X	X		X	X		X	X	X	X	X	X
BUSEMN																	
BVTEX															X		
CANARD	X	X		X	X	X	X		X	X		X		X		X	X
CCL			X														
CHRT8																	
CH1416																	
CLAM																	
CNT6																	
CNT11																	
CNT14																	
CNT15																	
CNT23																	
CNT31																	
CURVES													X		X		
EQ30																	
EQ31																	
FINTML			X														
FINTMR			X														
FINTNL			X														
FINTNR			X														
IBCIEU																	
ICSEVU																	
ICSICU																	
INFLU																	
INPT		X		X			X			X	X			X			
INT																	
INTFAC																	
LNTRP																	
NOSE	X	X		X		X	X		X						X		
REVFLO									X								
SHKAGL																	
SHKEXP											X						
SIMP1																	
SIMSON																	
VEL																	
WNGCNT																	
WNGCNW																	
XBAR								X									
XCPVSA								X			X						
YTAB																	

Figure A.3.- Common blocks in program.

Item 1 — Format(I5), 1 card

Column no.	5
Program variable	NCARDS

Format(20A4), NCARDS cards

Column no.	1 - 80
Program variable	HEAD

Item 2 — Format (9I5, 2L5), 1 card

Column no.	5	10	15	20	25	30	35	40
Program variable	NMACH	NDELT	NALFA	NPHI	NI	NNOSE	NCA	NVORT

45	50	55
NOUTPT	TURB	REFER

Item 3 — Format(8F10.5), 1 card

Column no.	10	20	30	40	50	60	70
Program variable	LROUT	SROUT	XMC	A	TIPRAD	ETAN	XCLE

Item 4 — Format (8F10.5), 1 card

Column no.	10	20	30	40	50
Program variable	CMACH(1)	CMACH(2)	CMACH(3)	CMACH(4)	CMACH(5)

(a) Page 1

Figure A.4.- Input formats for computer program.

Item 5 — Format(8F10.5), 1 card (omit if NCA = 0)

Column no.	10
Program variable	DCNDA

Item 6 — Format(8F10.5), 8 values of XNOSE per card

Column no.	10	20	. . .	10*NNOSE
Program variable	XNOSE(1)	XNOSE(2)	. . .	XNOSE(NNOSE)

Format(8F10.5), 8 values of RNOSE per card

Column no.	10	20	. . .	10*NNOSE
Program variable	RNOSE(1)	RNOSE(2)	. . .	RNOSE(NNOSE)

Item 7 — Format(8F10.5), 8 values of ALFAC per card

Column no.	10	20	. . .	10*NALFA
Program variable	ALFAC(1)	ALFAC(2)	. . .	ALFAC(NALFA)

(b) Page 2

Figure A.4.- Continued.

Item 8 — Format(8F10.5), 8 values of PHI per card

Column no.	10	20	. . .	10*NPHI
Program variable	PHI(1)	PHI(2)	. . .	PHI(NPHI)

Item 9 — Format(8F10.5), NDELT cards, J = 1, NDELT

Column no.	10	20	30	40
Program variable	DEFC(1,J)	DEFC(2,J)	DEFC(3,J)	DEFC(4,J)

Item 10 — Format(8F10.5), 1 card

Column no.	10	20	30	40
Program variable	SPANC	XCHL	XCTIPL	XCTE

Item 11 — Format (I5,2F10.5), 1 card

Column no.	5	15	25
Program variable	NFOILS	TOC	FOC

Item 12 — Format(I5), 1 card

Column no.	5
Program variable	999

(c) Page 3

Figure A.4.- Concluded.

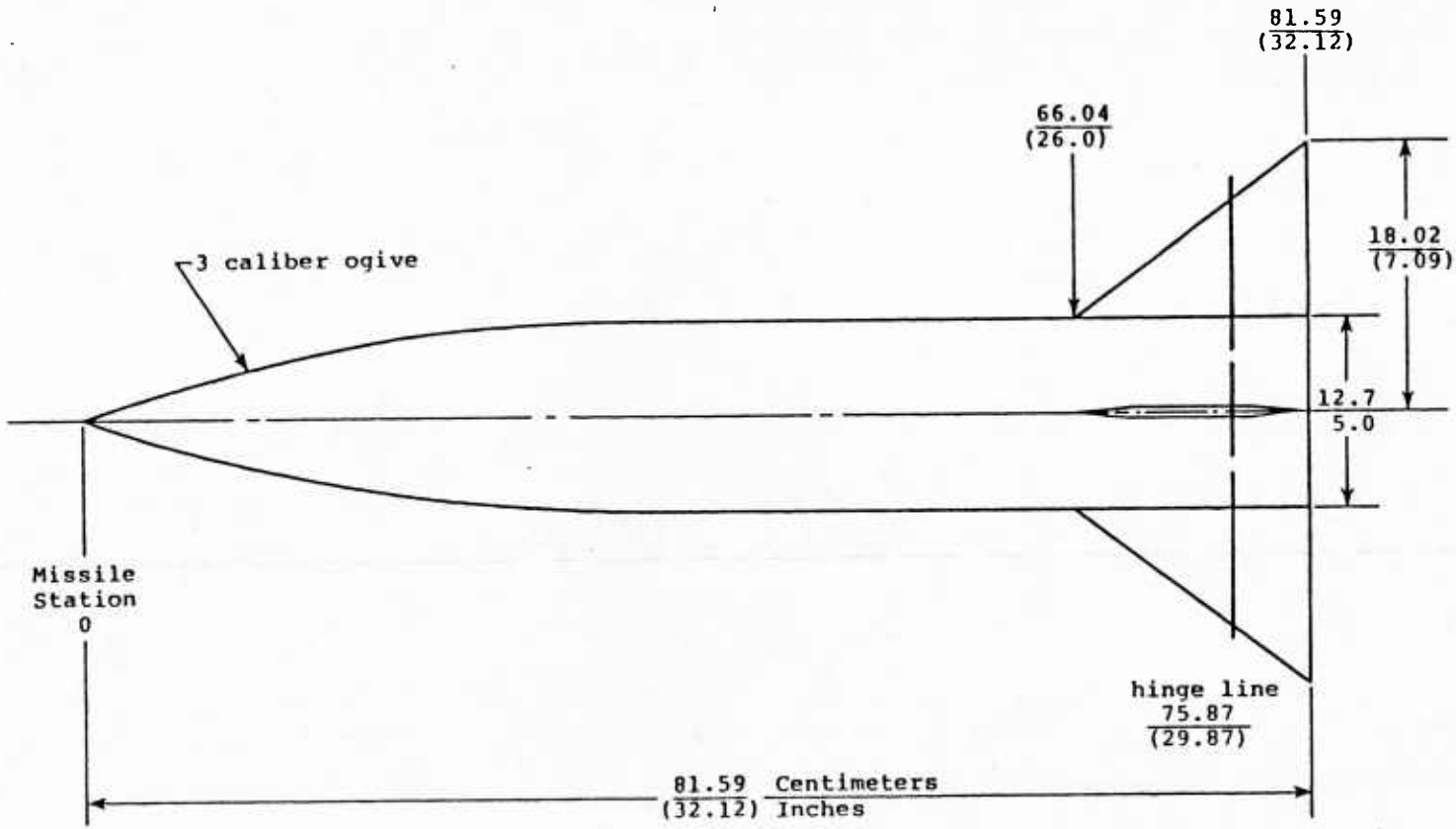

Figure A.5- Configuration used for sample case.

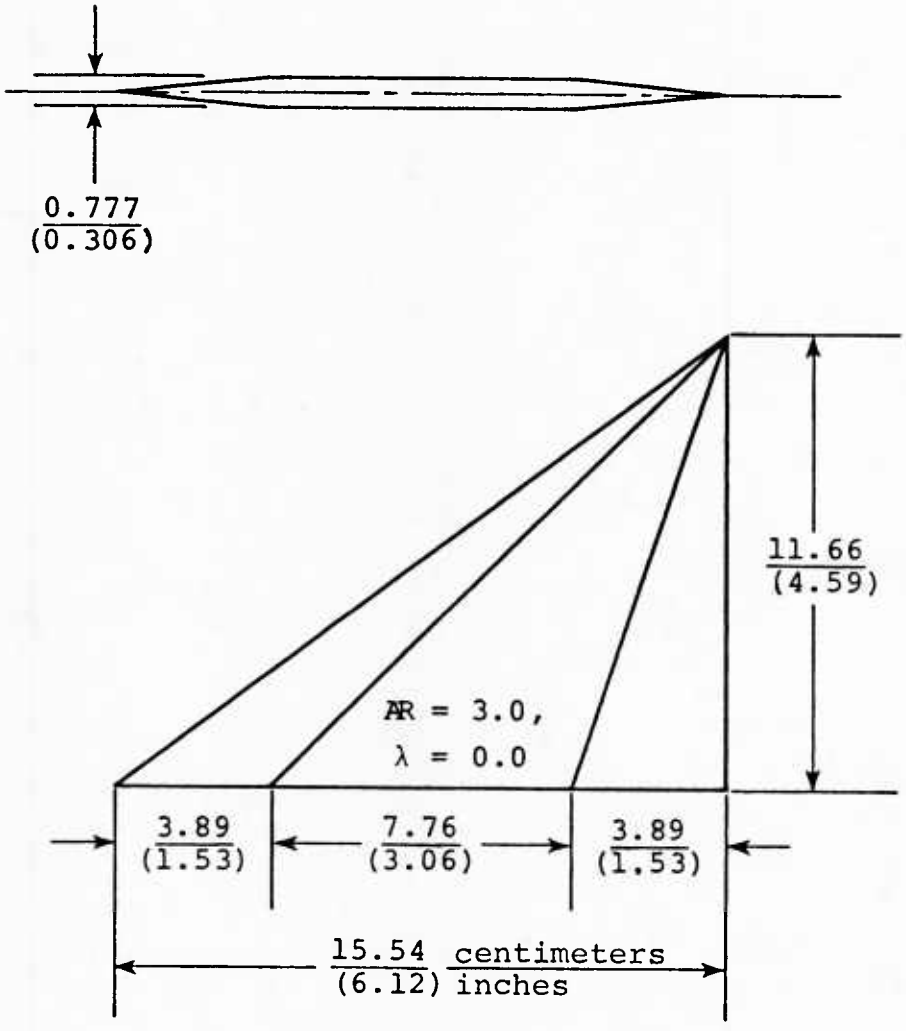

Figure A.6.- Dimensions of canard fins.

```
  10
PARAMETRIC HINGE MOMENT STUDY
BODY USED IS ARMY GENERALIZED MISSILE COMBINATION N1B
BODY TERMINATED AT CANARD TRAILING EDGE
CANARD ROOT CHORD LEADING EDGE AT MISSILE STATION 26.0
MACH NUMBERS 1.2, 1.6, 2.0, 2.5, 3.0
ANGLES OF ATTACK 0.01, 5.0, 10.0, 15.0, 20.0
FIN DEFLECTION ANGLES 0.0, 10.0, 20.0, -10.0, -20.0
ASPECT RATIO = 3.0, TAPER RATIO = 0.0, T/C = 0.05, F/C =0.5,  A/(S/2) = 0.3525
PHI = 0.0
HINGE LINE AT XHL/CR = 0.6322
   5    5    5    1   11   16    0    1    0    T    F
  5.0       19.635       0.0        2.5        0.0       17.8       26.0
  1.2        1.6         2.0        2.5        3.0
  0.0        1.673       2.0        2.5        3.0        4.0        5.0        6.0
  7.0        8.0         9.0       10.0       11.0       12.0       13.0       15.0
  0.0        0.537     0.635        0.779      0.916      1.173      1.406      1.616
  1.803      1.967       2.109      2.229      2.327      2.408      2.457      2.5
  0.01       5.0       10.0       15.0       20.0
  0.0
  0.0        0.0         0.0        0.0
  0.0       10.0         0.0       10.0
  0.0       20.0         0.0       20.0
  0.0      -10.0         0.0      -10.0
  0.0      -20.0         0.0      -20.0
  7.0928    29.8714    32.1237    32.1237
   6   0.05       0.5
 999
```

Figure A.7.- Input data for sample case.

```
                    CALCULATION OF AERODYNAMIC LOADS ON A CRUCIFORM MISSILE


                    PARAMETRIC HINGE MOMENT STUDY
                    BODY USED IS ARMY GENERALIZED MISSILE COMBINATION N1B
                    BODY TERMINATED AT CANARD TRAILING EDGE
                    CANARD ROOT CHORD LEADING EDGE AT MISSILE STATION 26.0
                    MACH NUMBERS 1.2, 1.6, 2.0, 2.5, 3.0
                    ANGLES OF ATTACK 0.01, 5.0, 10.0, 15.0, 20.0
                    FIN DEFLECTION ANGLES 0.0, 10.0, 20.0, -10.0, -20.0
                    ASPECT RATIO = 3.0, TAPER RATIO = 0.0, T/C = 0.05, F/C =0.5,  A/(S/2) = 0.3525
                    PHI = 0.0
                    HINGE LINE AT XHL/CR = 0.6322

********************************************************* MISSILE GEOMETRY *************************************************

                    MISSILE IS A BODY-TAIL COMBINATION OR FINNER

              *** NOSE GEOMETRY ***

   NOSE TIP RADIUS      NOSE HALF ANGLE      NOSE COORDINATES
                                              XNOSE       RNOSE
      0.00000             17.80000            0.000       0.000
                                              1.673        .537
                                              2.000        .635
                                              2.500        .779
                                              3.000        .916
                                              4.000       1.173
                                              5.000       1.406
                                              6.000       1.616
                                              7.000       1.803
                                              8.000       1.967
                                              9.000       2.109
                                             10.000       2.229
                                             11.000       2.327
                                             12.000       2.408
                                             13.000       2.457
                                             15.000       2.500

  LINEAR NORMAL FORCE COEFFICIENT SLOPE IS   2.000

             *** CANARD GEOMETRY ***

ASPECT RATIO        SEMISPAN       HINGE LINE      ROOT LEADING EDGE      TIP LEADING EDGE      TRAILING EDGE
    3.00002         7.09280        29.87140            26.00000              32.12370              32.12370

   THICKNESS MODEL DATA
     NUMBER OF AIRFOIL SECTIONS     6
     THICKNESS TO CHORD RATIO      .05000
     FLAT-SECTION LENGTH TO CHORD RATIO     .50000

             *** BODY GEOMETRY ***

       BODY RADIUS          BODY LENGTH
         2.500                32.124

************************************************  REFERENCE LENGTHS AND AREAS  ************************************************

            REFERENCE LENGTHS                                  REFERENCE AREAS
       OUTPUT LENGTH =    4.00000                      OUTPUT AREA =   19.63500
       CPXRC =    4.12370     CPYRC =    4.59280       CANARD WING-ALONE REF. AREA =   28.12493

       MOMENT CENTER IS AT X =  0.000

*************************************************  FLIGHT CONDITIONS  *************************************************

   TURBULENT FLOW
         T

   CANARD DEFLECTION ANGLES
                  FIN NO.        1         2         3         4
                                0.00      0.00      0.00      0.00
                                0.00     10.00      0.00     10.00
                                0.00     20.00      0.00     20.00
                                0.00    -10.00      0.00    -10.00
                                0.00    -20.00      0.00    -20.00

      MACH NUMBERS      1.20      1.60      2.00      2.50      3.00
  ANGLES OF ATTACK       .01      5.00     10.00     15.00     20.00
       ROLL ANGLES      0.00

*************************************************  PROGRAM OPERATION  *************************************************

    NI   NCA  NOUTPT  REFER  NVORT
    11    0      0      F      1

 NOSE VORTICES ARE RUN TO CANARD LEADING EDGE
```

(a) Input Data

Figure A.8.- Output for sample case.

********** MACH NUMBER = 1.20 **********

FIN-ALONE NORMAL-FORCE CURVE (REFERENCE AREA IS PLANFORM AREA OF ONE FIN)

ALPHA	CNW
0.0	0.000
2.0	.124
4.0	.247
6.0	.369
8.0	.485
10.0	.593
12.0	.692
14.0	.784
16.0	.866
18.0	.940
20.0	1.008
22.0	1.071
24.0	1.127
26.0	1.178
28.0	1.225
30.0	1.268
32.0	1.309
34.0	1.348
36.0	1.386
38.0	1.422
40.0	1.456
42.0	1.489
44.0	1.518
46.0	1.549
48.0	1.580
50.0	1.610
52.0	1.640
54.0	1.669
56.0	1.694
58.0	1.718
60.0	1.738

CHORDWISE CENTER-OF-PRESSURE LOCATION

ALPHA	XBAR/CR	THICKNESS CORRECTION
2.0	.61518	BUSEMANN
45.0	.64800	DATA BASE

(b) Fin alone normal force and center of pressure

Figure A.8.- (Continued).

THE FOLLOWING CALCULATIONS ARE FOR
MACH NUMBER = 1.20
DELTAC1 = 0.00
DELTAC2 = 0.00
DELTAC3 = 0.00
DELTAC4 = 0.00
ROLL ANGLE = 0.00

********** CANARD SECTION RESULTS FOR ALPHA = .010 AND PHI = 0.000 **********

	***** CANARD FIN VORTEX LOADS *****						***** TOTAL CANARD FIN LOADS ***** (LOADS ARE BASED ON SROUT AND LROUT)				
PANEL	(DALFEQ)V	(DCN)V	(DCBM)V	(DCHM)V	(DCRM)V		ALFEQ	CNF	CBM	CHM	CRM	XCPCR
1	0.00	0.0000	0.0000	0.0000	0.0000	*	-.00	-.0000	-.0000	-.0000	-.0000	.6136
2	0.00	0.0000	0.0000	0.0000	0.0000	*	.01	.0005	.0002	.0000	.0005	.6137
3	0.00	0.0000	0.0000	0.0000	0.0000	*	-.00	-.0000	-.0000	-.0000	-.0000	.6136
4	0.00	0.0000	0.0000	0.0000	0.0000	*	.01	.0005	.0002	.0000	.0005	.6137

********** CANARD SECTION RESULTS FOR ALPHA = 5.000 AND PHI = 0.000 **********

	***** CANARD FIN VORTEX LOADS *****						***** TOTAL CANARD FIN LOADS ***** (LOADS ARE BASED ON SROUT AND LROUT)				
PANEL	(DALFEQ)V	(DCN)V	(DCBM)V	(DCHM)V	(DCRM)V		ALFEQ	CNF	CBM	CHM	CRM	XCPCR
1	0.00	0.0000	0.0000	0.0000	0.0000	*	-.00	-.0000	-.0000	-.0000	-.0000	.6136
2	0.00	0.0000	0.0000	0.0000	0.0000	*	6.02	.2648	.0976	.0045	.2300	.6182
3	0.00	0.0000	0.0000	0.0000	0.0000	*	-.00	-.0000	-.0000	-.0000	-.0000	.6136
4	0.00	0.0000	0.0000	0.0000	0.0000	*	6.02	.2648	.0976	.0045	.2300	.6182

********** CANARD SECTION RESULTS FOR ALPHA = 10.000 AND PHI = 0.000 **********

	***** CANARD FIN VORTEX LOADS *****						***** TOTAL CANARD FIN LOADS ***** (LOADS ARE BASED ON SROUT AND LROUT)				
PANEL	(DALFEQ)V	(DCN)V	(DCBM)V	(DCHM)V	(DCRM)V		ALFEQ	CNF	CBM	CHM	CRM	XCPCR
1	0.00	0.0000	0.0000	0.0000	0.0000	*	-.00	-.0000	-.0000	-.0000	-.0000	.6136
2	0.00	0.0000	0.0000	0.0000	0.0000	*	12.22	.5029	.1714	.0057	.4228	.6230
3	0.00	0.0000	0.0000	0.0000	0.0000	*	-.00	-.0000	-.0000	-.0000	-.0000	.6136
4	0.00	0.0000	0.0000	0.0000	0.0000	*	12.22	.5029	.1714	.0057	.4228	.6230

********** CANARD SECTION RESULTS FOR ALPHA = 15.000 AND PHI = 0.000 **********

	***** CANARD FIN VORTEX LOADS *****						***** TOTAL CANARD FIN LOADS ***** (LOADS ARE BASED ON SROUT AND LROUT)				
PANEL	(DALFEQ)V	(DCN)V	(DCBM)V	(DCHM)V	(DCRM)V		ALFEQ	CNF	CBM	CHM	CRM	XCPCR
1	0.00	0.0000	0.0000	0.0000	0.0000	*	-.00	-.0000	-.0000	-.0000	-.0000	.6136
2	0.00	0.0000	0.0000	0.0000	0.0000	*	17.79	.6677	.2193	.0041	.5531	.6272
3	0.00	0.0000	0.0000	0.0000	0.0000	*	-.00	-.0000	-.0000	-.0000	-.0000	.6136
4	0.00	0.0000	0.0000	0.0000	0.0000	*	17.79	.6677	.2193	.0041	.5531	.6272

********** CANARD SECTION RESULTS FOR ALPHA = 20.000 AND PHI = 0.000 **********

	***** CANARD FIN VORTEX LOADS *****						***** TOTAL CANARD FIN LOADS ***** (LOADS ARE BASED ON SROUT AND LROUT)				
PANEL	(DALFEQ)V	(DCN)V	(DCBM)V	(DCHM)V	(DCRM)V		ALFEQ	CNF	CBM	CHM	CRM	XCPCR
1	0.00	0.0000	0.0000	0.0000	0.0000	*	-.00	-.0000	-.0000	-.0000	-.0000	.6136
2	0.00	0.0000	0.0000	0.0000	0.0000	*	22.75	.7820	.2492	.0011	.6402	.6310
3	0.00	0.0000	0.0000	0.0000	0.0000	*	-.00	-.0000	-.0000	-.0000	-.0000	.6136
4	0.00	0.0000	0.0000	0.0000	0.0000	*	22.75	.7820	.2492	.0011	.6402	.6310

(c) Canard fin forces and moments for NOUTPT = 0

Figure A.8.- (Continued).

THE FOLLOWING CALCULATIONS ARE FOR

MACH NUMBER = 1.20
DELTAC1 = 0.00
DELTAC2 = 0.00
DELTAC3 = 0.00
DELTAC4 = 0.00
ROLL ANGLE = 0.00

******************************* CONTRIBUTION OF NOSE SECTION TO TOTAL LOADS FOR ALPHA = 20.00 *******************************

STRENGTHS AND POSITIONS OF VORTICES AT LEADING EDGE OF CANARD ROOT CHORD

I	GAMMA/2PIVA	YO/A	ZO/A
1	.15126	.7856	1.5446
2	-.15126	-.7856	1.5446

NORMAL-FORCE, PITCHING-MOMENT, LIFT, AND DRAG COEFFICIENTS
IN UNROLLED BODY COORDINATES (BASED ON SROUT AND LROUT)

CZO	CMYO	CL	CD
1.30596	-2.84012	1.22720	.44666

******************************* CANARD SECTION RESULTS FOR ALPHA = 20.000 AND PHI = 0.000 *******************************

***** CANARD FIN VORTEX LOADS ***** ***** TOTAL CANARD FIN LOADS *****
(LOADS ARE BASED ON SROUT AND LROUT)

PANEL	(DALFEQ)V	(DCN)V	(DCBM)V	(DCHM)V	(DCRM)V		ALFEQ	CNF	CBM	CHM	CRM	XCPCR
1	0.00	0.0000	0.0000	0.0000	0.0000	*	-.00	-.0000	-.0000	-.0000	-.0000	.6136
2	0.00	0.0000	0.0000	0.0000	0.0000	*	22.75	.7820	.2492	.0011	.6402	.6310
3	0.00	0.0000	0.0000	0.0000	0.0000	*	-.00	-.0000	-.0000	-.0000	-.0000	.6136
4	0.00	0.0000	0.0000	0.0000	0.0000	*	22.75	.7820	.2492	.0011	.6402	.6310

EFFECT OF HINGE-LINE LOCATION ON HINGE MOMENT
HINGE MOMENTS

XHL/CR	FIN 1	FIN 2	FIN 3	FIN 4
.2000	.0000	-.4128	.0000	-.4128
.3000	.0000	-.3170	.0000	-.3170
.4000	.0000	-.2213	.0000	-.2213
.5000	.0000	-.1255	.0000	-.1255
.6000	.0000	-.0297	.0000	-.0297
.7000	-.0000	.0661	-.0000	.0661
.8000	-.0000	.1618	-.0000	.1618

*** TOTAL CANARD FIN LOADS BASED ON PLANFORM AREA, ROOT CHORD, AND EXPOSED SEMISPAN ***

PANEL	ALFEQ	CNF	CBM	CHM	CRM
1	-.00	-.0000	-.0000	-.0000	-.0000
2	22.75	1.0919	.3788	.0013	.9731
3	-.00	-.0000	-.0000	-.0000	-.0000
4	22.75	1.0919	.3788	.0013	.9731

*** CONTRIBUTION OF CANARD SECTION TO TOTAL LOADS ***
(LOADS ARE BASED ON SROUT AND LROUT)

UNROLLED COORDINATES

CXO = 0.0000 CMXO = 0.0000
CYO = .0000 CMYO = -11.6539
CZO = 1.9502 CMZO = .0000
CL = 1.8325
CD = .6670

ROLLED COORDINATES

CX = 0.0000 CMX = 0.0000
CY = .0000 CMY = -11.6539
CZ = 1.9502 CMZ = .0000

*** SUMMARY OF TOTAL LOADS ***
ALPHA = 20.00 PHI = 0.00

UNROLLED COORDINATES *** BODY AXIS COORDINATES

	CXO	CYO	CZO	CMXO	CMYO	CMZO	CX	CY	CZ	CMX	CMY	CMZ
NOSE	0.00000	0.00000	1.30596	0.00000	-2.84012	0.00000	0.00000	0.00000	1.30596	0.00000	-2.84012	0.00000
CANARD	0.00000	.00000	1.95015	0.00000	-11.65393	.00000	0.00000	.00000	1.95015	0.00000	-11.65393	.00000
TOTALS	0.00000	.00000	3.25611	0.00000	-14.49405	.00000	0.00000	.00000	3.25611	0.00000	-14.49405	.00000

AXIAL CENTERS OF PRESSURE

NORMAL FORCE (CPX) = 4.45134
SIDE FORCE (CPY) = 5.96042

(d) Forces and moments for NOUTPT = 1

Figure A.8.- (Continued).

MAXIMUM AND MINIMUM HINGE MOMENTS FOR FIN 4 (BASED ON SROUT AND LROUT), OVER THE RANGES OF ANGLE OF ATTACK AND FIN DEFLECTION ANGLE FOR WHICH CALCULATIONS WERE MADE, FOR A GIVEN ROLL ANGLE, THEY ARE TABULATED AS A FUNCTION OF HINGE-LINE LOCATION AND MACH NUMBER.

ROLL ANGLE (PHI) = 0.00

********** MAXIMUM HINGE MOMENT **********						********** MINIMUM HINGE MOMENT **********					
XHL/CR	M=1.20	M=1.60	M=2.00	M=2.50	M=3.00	XHL/CR	M=1.20	M=1.60	M=2.00	M=2.50	M=3.00
.20	.3461	.3801	.4078	.4529	.4944	.20	-.5706	-.6246	-.7077	-.8252	-.9436
.21	.3379	.3713	.3984	.4424	.4829	.21	-.5577	-.6099	-.6910	-.8059	-.9219
.22	.3298	.3626	.3890	.4320	.4714	.22	-.5449	-.5953	-.6743	-.7867	-.9003
.23	.3216	.3538	.3796	.4216	.4599	.23	-.5321	-.5806	-.6575	-.7674	-.8786
.24	.3135	.3450	.3702	.4111	.4484	.24	-.5192	-.5659	-.6408	-.7481	-.8570
.25	.3054	.3363	.3608	.4007	.4369	.25	-.5064	-.5513	-.6241	-.7289	-.8353
.26	.2972	.3275	.3515	.3902	.4254	.26	-.4936	-.5366	-.6074	-.7096	-.8137
.27	.2891	.3188	.3421	.3798	.4139	.27	-.4807	-.5219	-.5907	-.6903	-.7920
.28	.2809	.3100	.3327	.3693	.4024	.28	-.4679	-.5073	-.5739	-.6711	-.7704
.29	.2728	.3012	.3233	.3589	.3909	.29	-.4551	-.4926	-.5572	-.6518	-.7487
.30	.2647	.2925	.3139	.3484	.3793	.30	-.4422	-.4779	-.5405	-.6325	-.7271
.31	.2565	.2837	.3045	.3380	.3678	.31	-.4294	-.4633	-.5238	-.6133	-.7054
.32	.2484	.2749	.2951	.3275	.3563	.32	-.4165	-.4486	-.5071	-.5940	-.6838
.33	.2402	.2662	.2857	.3171	.3448	.33	-.4037	-.4339	-.4903	-.5747	-.6621
.34	.2321	.2574	.2764	.3066	.3333	.34	-.3909	-.4193	-.4736	-.5554	-.6405
.35	.2239	.2486	.2670	.2962	.3218	.35	-.3780	-.4046	-.4569	-.5362	-.6188
.36	.2158	.2399	.2576	.2857	.3103	.36	-.3652	-.3899	-.4402	-.5169	-.5972
.37	.2077	.2311	.2482	.2753	.2988	.37	-.3524	-.3753	-.4235	-.4976	-.5755
.38	.1995	.2224	.2388	.2648	.2873	.38	-.3395	-.3606	-.4067	-.4784	-.5539
.39	.1914	.2136	.2294	.2544	.2758	.39	-.3267	-.3459	-.3900	-.4591	-.5322
.40	.1832	.2048	.2200	.2440	.2643	.40	-.3139	-.3313	-.3733	-.4398	-.5106
.41	.1751	.1961	.2106	.2335	.2528	.41	-.3010	-.3166	-.3566	-.4206	-.4889
.42	.1670	.1873	.2013	.2231	.2413	.42	-.2882	-.3019	-.3399	-.4013	-.4673
.43	.1588	.1785	.1919	.2126	.2298	.43	-.2754	-.2873	-.3231	-.3820	-.4457
.44	.1507	.1698	.1825	.2022	.2182	.44	-.2625	-.2726	-.3064	-.3628	-.4240
.45	.1425	.1610	.1731	.1917	.2067	.45	-.2497	-.2579	-.2897	-.3435	-.4024
.46	.1344	.1522	.1637	.1813	.1952	.46	-.2368	-.2433	-.2730	-.3242	-.3807
.47	.1263	.1435	.1543	.1708	.1837	.47	-.2240	-.2286	-.2563	-.3050	-.3591
.48	.1181	.1347	.1449	.1604	.1722	.48	-.2112	-.2139	-.2395	-.2857	-.3374
.49	.1100	.1260	.1356	.1499	.1607	.49	-.1983	-.1993	-.2228	-.2664	-.3158
.50	.1018	.1172	.1262	.1395	.1492	.50	-.1855	-.1846	-.2061	-.2471	-.2941
.51	.0937	.1084	.1168	.1290	.1377	.51	-.1727	-.1699	-.1894	-.2279	-.2725
.52	.0856	.0997	.1074	.1186	.1262	.52	-.1598	-.1553	-.1727	-.2086	-.2508
.53	.0774	.0909	.0980	.1081	.1147	.53	-.1470	-.1406	-.1559	-.1893	-.2292
.54	.0693	.0821	.0886	.0977	.1032	.54	-.1342	-.1259	-.1392	-.1701	-.2075
.55	.0611	.0734	.0792	.0873	.0917	.55	-.1213	-.1113	-.1225	-.1508	-.1859
.56	.0530	.0646	.0698	.0768	.0802	.56	-.1085	-.0966	-.1058	-.1315	-.1642
.57	.0449	.0558	.0605	.0664	.0687	.57	-.0956	-.0819	-.0891	-.1123	-.1426
.58	.0367	.0471	.0511	.0559	.0571	.58	-.0828	-.0673	-.0734	-.0943	-.1209
.59	.0286	.0383	.0417	.0455	.0456	.59	-.0700	-.0526	-.0577	-.0763	-.0995
.60	.0204	.0296	.0323	.0350	.0341	.60	-.0571	-.0383	-.0434	-.0596	-.0795
.61	.0123	.0208	.0229	.0246	.0254	.61	-.0443	-.0248	-.0300	-.0439	-.0595
.62	.0042	.0120	.0140	.0158	.0172	.62	-.0315	-.0129	-.0182	-.0295	-.0394
.63	.0045	.0061	.0113	.0085	.0089	.63	-.0186	-.0039	-.0091	-.0156	-.0194
.64	.0108	.0208	.0280	.0226	.0090	.64	-.0121	-.0055	-.0052	-.0068	-.0119
.65	.0186	.0354	.0447	.0419	.0306	.65	-.0203	-.0143	-.0146	-.0172	-.0234
.66	.0278	.0501	.0614	.0612	.0523	.66	-.0284	-.0230	-.0240	-.0277	-.0349
.67	.0377	.0648	.0781	.0804	.0739	.67	-.0365	-.0318	-.0334	-.0381	-.0464
.68	.0483	.0794	.0949	.0997	.0956	.68	-.0447	-.0406	-.0428	-.0486	-.0579
.69	.0596	.0941	.1116	.1190	.1172	.69	-.0528	-.0493	-.0522	-.0590	-.0694
.70	.0716	.1088	.1283	.1382	.1389	.70	-.0610	-.0581	-.0616	-.0694	-.0809
.71	.0841	.1234	.1450	.1575	.1605	.71	-.0691	-.0668	-.0710	-.0799	-.0925
.72	.0969	.1381	.1617	.1768	.1821	.72	-.0772	-.0756	-.0803	-.0903	-.1040
.73	.1097	.1528	.1785	.1960	.2038	.73	-.0854	-.0844	-.0897	-.1008	-.1155
.74	.1226	.1674	.1952	.2153	.2254	.74	-.0935	-.0931	-.0991	-.1112	-.1270
.75	.1354	.1821	.2119	.2346	.2471	.75	-.1017	-.1019	-.1085	-.1217	-.1385
.76	.1482	.1968	.2286	.2538	.2687	.76	-.1098	-.1107	-.1179	-.1321	-.1500
.77	.1611	.2114	.2453	.2731	.2904	.77	-.1180	-.1194	-.1273	-.1426	-.1615
.78	.1739	.2261	.2621	.2924	.3120	.78	-.1261	-.1282	-.1367	-.1530	-.1730
.79	.1867	.2408	.2788	.3117	.3337	.79	-.1342	-.1370	-.1461	-.1635	-.1845
.80	.1996	.2554	.2955	.3309	.3553	.80	-.1424	-.1457	-.1554	-.1739	-.1960

END OF CALCULATIONS FOR THIS CASE

(e) Summary of maximum and mimimum hinge moments

Figure A.8.- (Concluded).

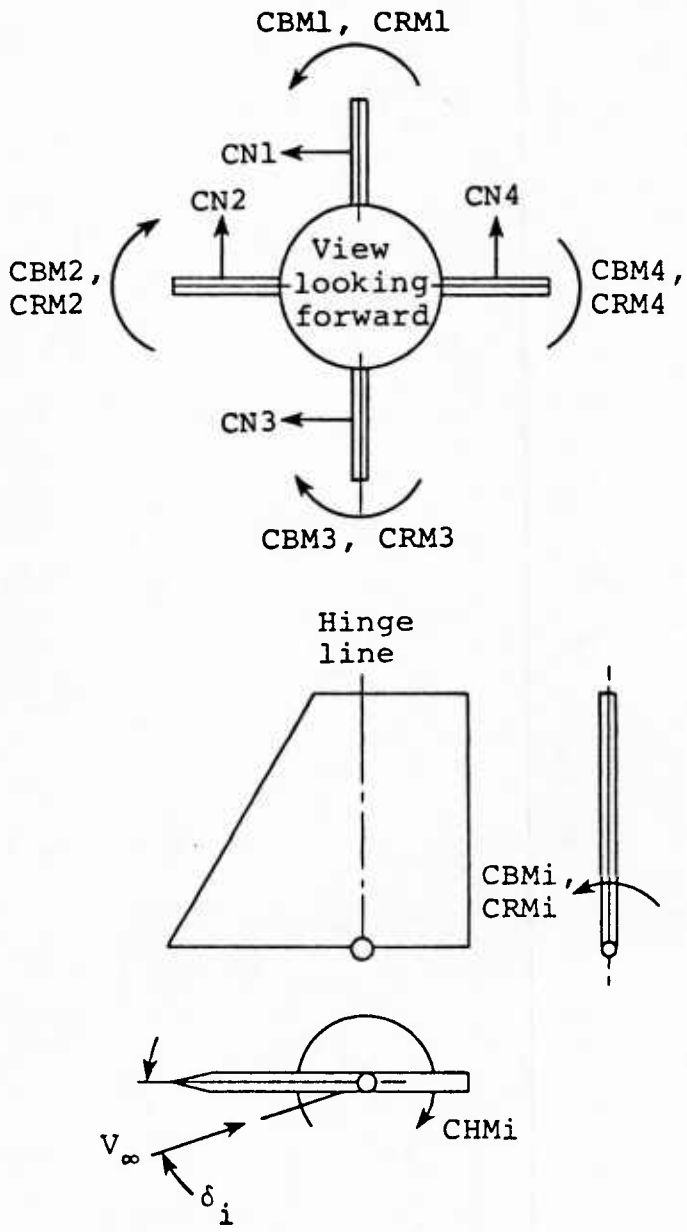

Figure A.9.- Positive directions for canard fin force and moment coefficients.

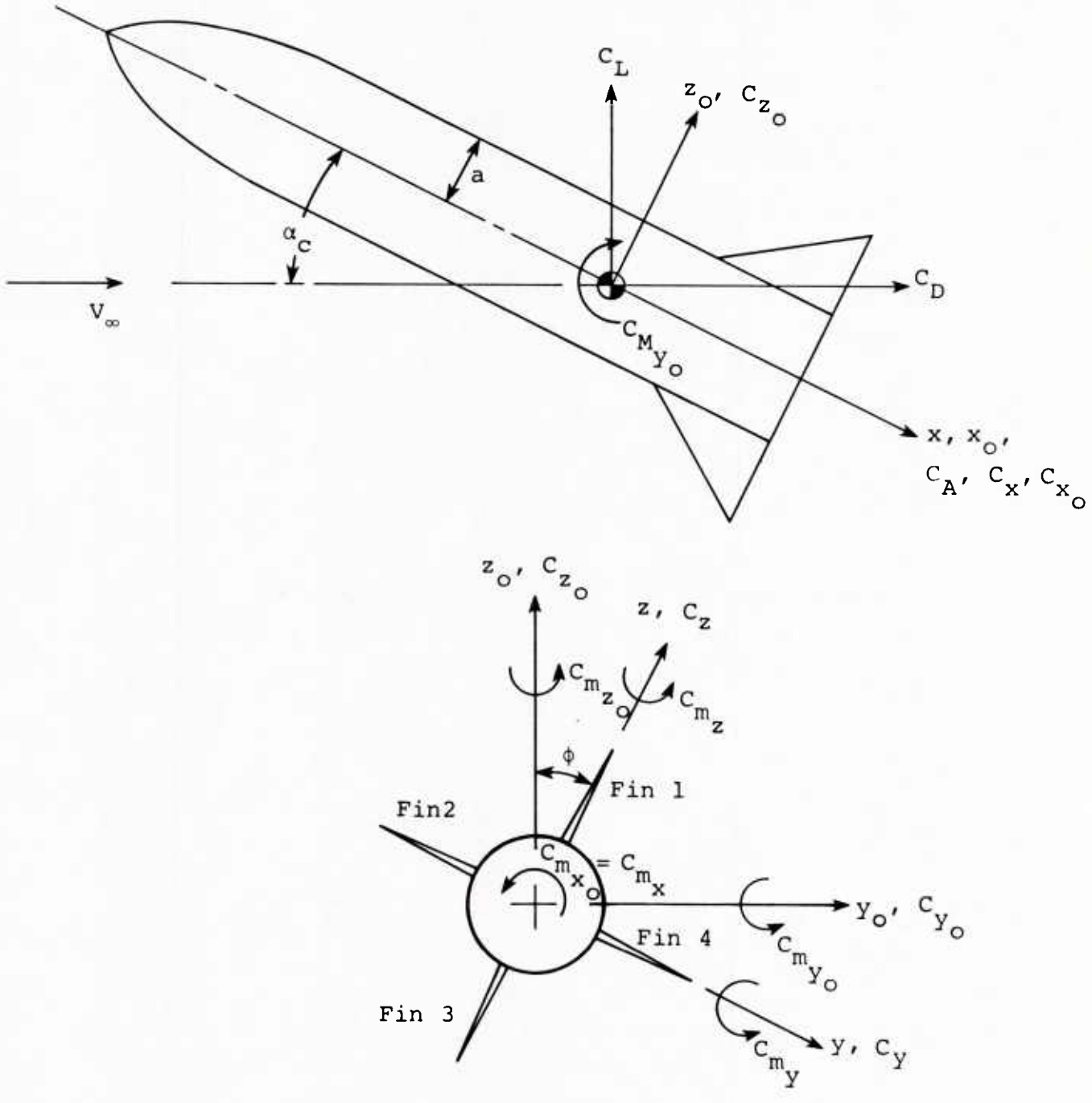

Figure A.10- Unrolled (x_o, y_o, z_o,) and rolled (x, y, z) coordinate systems and positive directions of forces and moments in the two systems..

REFERENCES

A1. Nielsen, J. N., Hemsch, M. J., and Smith, C. A.: A Preliminary Method for Calculating the Aerodynamic Characteristics of Cruciform Missiles to High Angles of Attack Including Effects of Roll Angle and Control Deflections. Office of Naval Research, Report ONR-CR215-226-4F, Nov. 1977 (also NEAR TR 152).

A2. Smith, C. A. and Nielsen, J. N.: Prediction of Aerodynamic Characteristics of Cruciform Missiles to High Angles of Attack Utilizing a Distributed Vortex Wake. NEAR TR 208, Jan. 1980. (MISSILE 2)

A3. Nielsen, J. N. and Goodwin, F. K.: Preliminary Method for Estimating Hinge Moments of All-Movable Controls. NEAR TR 268, Mar. 1982.

A4. Nielsen, J. N.: Missile Aerodynamics. McGraw-Hill Book Co., 1960.

A5. Pitts, W. C. Nielsen, J. N., and Kaattari, G. E.: Lift and Center of Pressure of Wing-Body-Tail Combinations at Subsonic, Transonic, and Supersonic Speeds. NACA Report 1307, 1957.

A6. Mendenhall, M. R., Goodwin, F. K., Dillenius, M. F. E., and Kline, D. M.: Computer Programs for Calculating the Static Longitudinal Aerodynamic Characteristics of Wing-Body-Tail Configurations. NASA CR-2474, 1975.

A7. Hemsch, M. J. and Nielsen, J. N.: Test Report for Canard Missile Tests in Ames 6- by 6-Foot Supersonic Wind Tunnel. NEAR TR 72, 1974.

A8. Hemsch, M. J.: Reduced Vapor Screen Data from Canard Missile Tests in Ames 6- by 6-Foot Supersonic Wind Tunnel. NEAR TR 81, 1975.